Radar Clutter Modeling

Maria S. GRECO and Fulvio GINI
Dipartimento di Ingegneria dell'Informazione
University of Pisa
Via G. Caruso 16, I-56122, Pisa, Italy
m.greco@iet.unipi.it

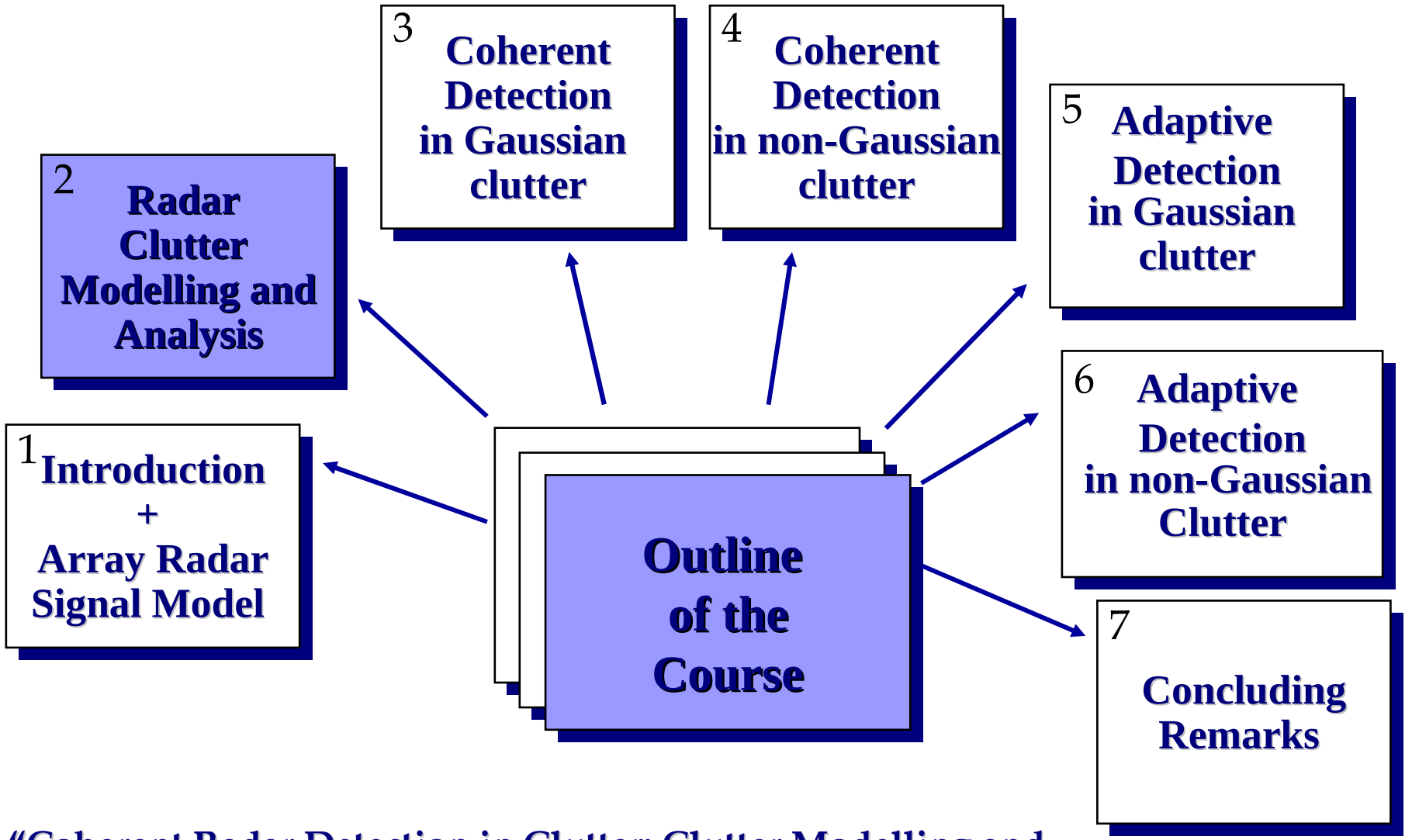

"Coherent Radar Detection in Clutter: Clutter Modelling and Analysis + Adaptive Array Radar Signal Processing"

What is the clutter?

Clutter refers to radio frequency (RF) echoes returned from targets which are uninteresting to the radar operators and interfere with the observation of useful signals.

Such targets include natural objects such as ground, sea, precipitations (rain, snow or hail), sand storms, animals (especially birds), atmospheric turbulence, and other atmospheric effects, such as ionosphere reflections and meteor trails.

Clutter may also be returned from man-made objects such as buildings and, intentionally, by radar countermeasures such as chaff.

Clutter reflectivity: General Concepts

We will focus particularly on sea and land (or ground) clutter

- Radar cross section (RCS)
- RCS per unit illuminated area, σ^o (m^2/m^2)
- RCS per unit illuminated volume, η (m^2/m^3)
- Radar equation and pattern-propagation factor F
- Sea clutter RCS and spikes
- Land clutter RCS
- Sea and land clutter statistics
- The compound-Gaussian model
- Clutter spectral models

Clutter reflectivity

A perfectly smooth and flat conducting surface acts as a mirror, producing a coherent forward reflection, with the angle of incidence equal to the angle of reflection. If the surface has some roughness, the forward scatter component is reduced by diffuse, non-coherent scattering in other directions.

For monostatic radar, clutter is the diffuse backscatter in the direction towards the radar

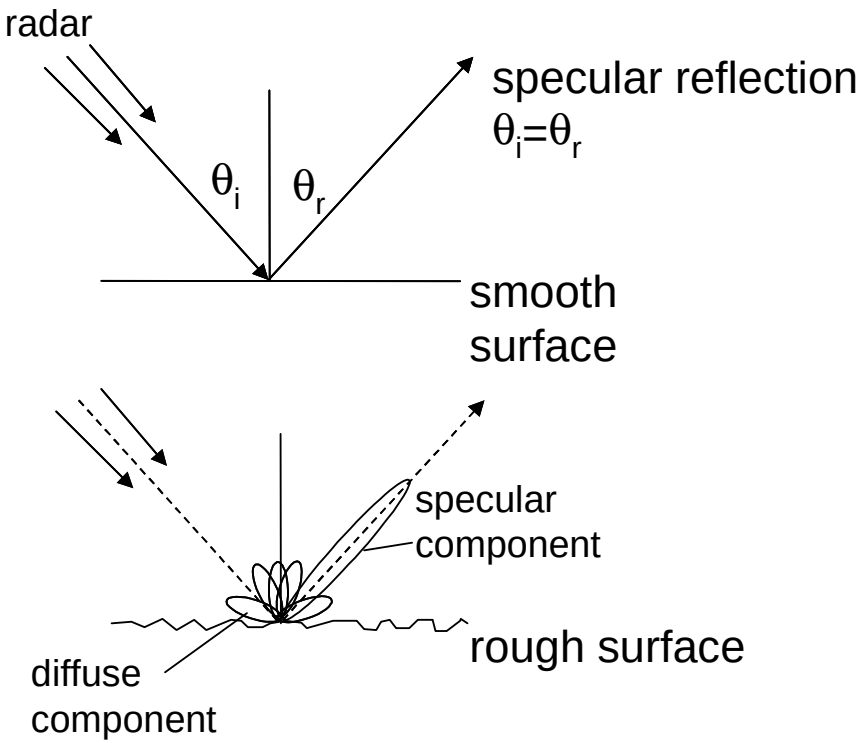

Radar Cross Section (RCS)

- The IEEE Standard for RCS in square meters is

$$\sigma = 4\pi \frac{P_s}{\Omega p_i}$$

where

P_s = power (watts) scattered in a specified direction from the target having RCS σ

Ω = solid angle (steradians) over which P_s is scattered

p_i = power density (watts/m^2) of plane wave at target

Radar Cross Section (RCS)

Range of RCS Values (dBm^2)

- Echo power directly proportional to RCS
- Factors that influence RCS:

  size, shape, material composition, moisture content, surface coating and roughness, orientation, polarization, wavelength, multipath

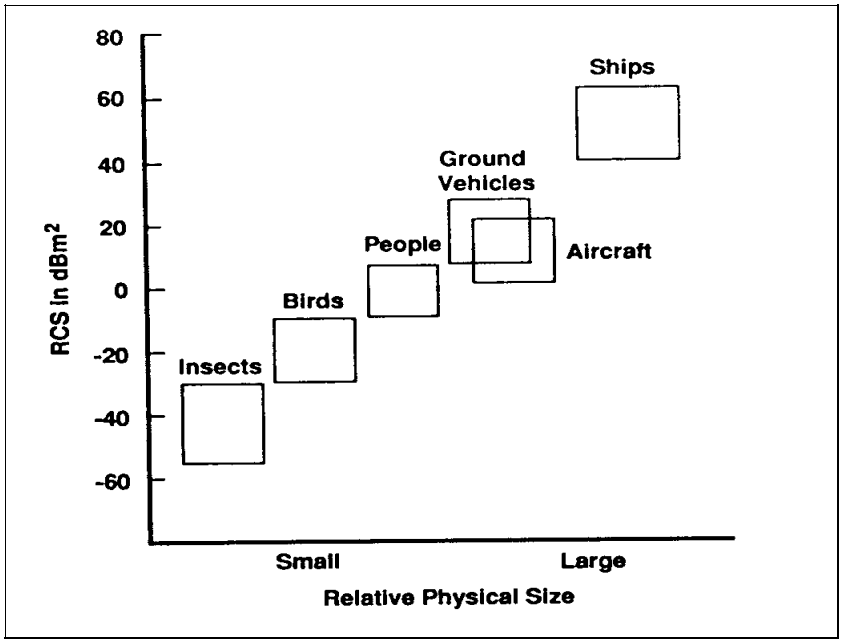

RCS of common objects

Normalized RCS σ_0

The normalized clutter reflectivity, σ_0, is defined as the total RCS, σ, of the scatterers in the illuminated patch, normalized by the area, A_c, of the patch and it is measured in units of dBm^2/m^2.

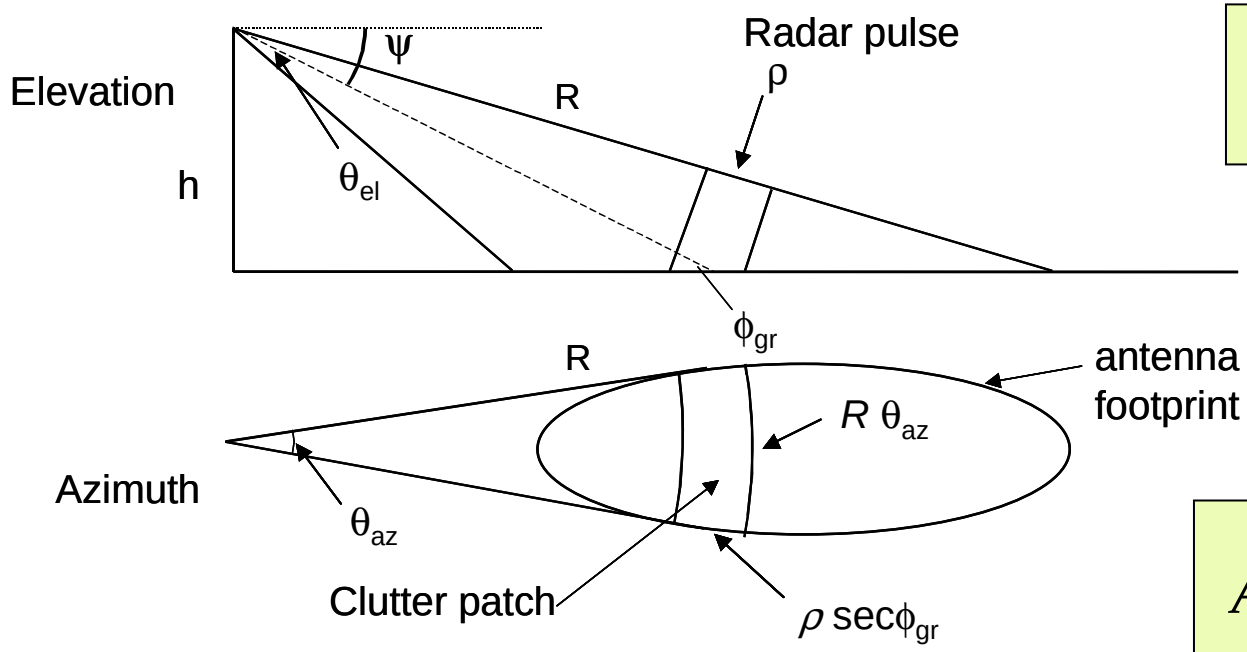

$$\sigma^0 = \sigma / A_c$$

range resolution

$$A_c = \alpha \rho R \theta_{az} \sec(\phi_{gr})$$

local grazing angle

The factor α accounts for the actual compressed pulse shape and the azimuth beamshape

Volume reflectivity η

The volume clutter reflectivity, η, is defined as the total RCS, σ, of the scatterers in the illuminated volume, normalized by the volume itself, V_c, and it is measured in units of dBm^2/m^3.

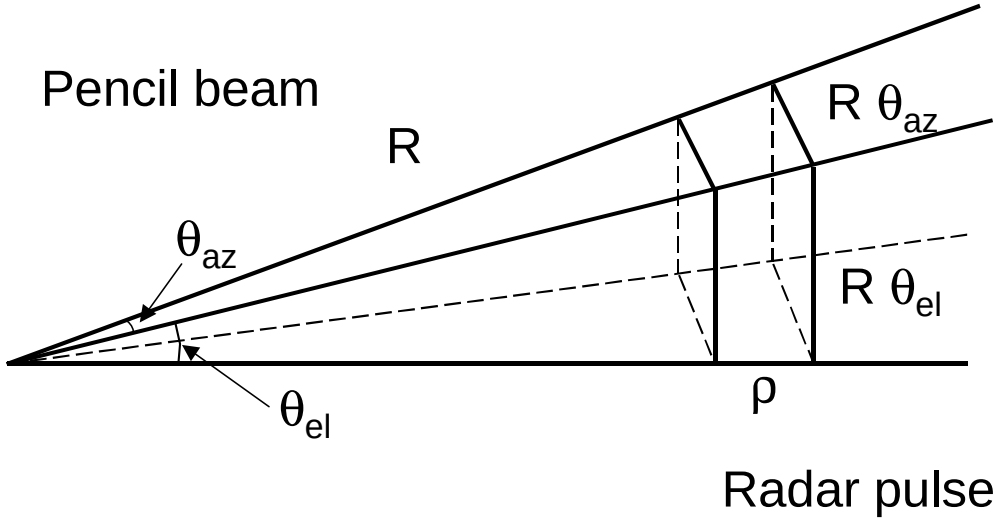

$$\eta = \sigma / V_c$$

$$V_c = \alpha \rho R^2 \theta_{az} \theta_{el}$$

→ one-way 3dB elevation beamwidth

Radar Equation and propagation factor F

- For monostatic radar, received power P_r from a target with RCS σ is

$$P_r = \frac{P_t G^2 \lambda^2}{(4\pi)^3 R^4} \sigma F^4$$

- P_t = transmit power
- G = antenna gain
- R = distance of target from antenna
- F = the pattern-propagation factor, the ratio of field strength at a point to that which would be present if free-space propagation had occurred

A clutter measurement provides either σF^4 or $\sigma^o F^4$.
Even so, normally the data are reported as being σ or σ^o.

Discrete and distributed clutter

DISCRETE

- RCS depends on aspect angle, multipath environment, frequency, and polarization
- RCS values up to 30 dBm^2 are common
- RCS above 40 dBm^2 rare, except in built-up areas
- Nominal RCS values:

60 dBm^2	very large ship or building
50/40 dBm^2	large building or ship
30/20 dBm^2	small building/house
20/10 dBm^2	trucks/automobiles

DISTRIBUTED

- Average RCS = s^o times A, where A is illuminated surface area (footprint) of a range-azimuth cell

Sea clutter: Dependence on grazing angle

At near vertical incidence, the backscatter is quasi-specular and varies inversely with surface roughness with a maximum at vertical incidence for a perfectly smooth surface.

At medium grazing angles the reflectivity shows a lower dependence on grazing angle (plateau region).

Below some critical angle (~ 10°, depending on the roughness) the reflectivity reduces rapidly with smaller grazing angles (interference region, where propagation is strongly affected by multipath scattering and shadowing).

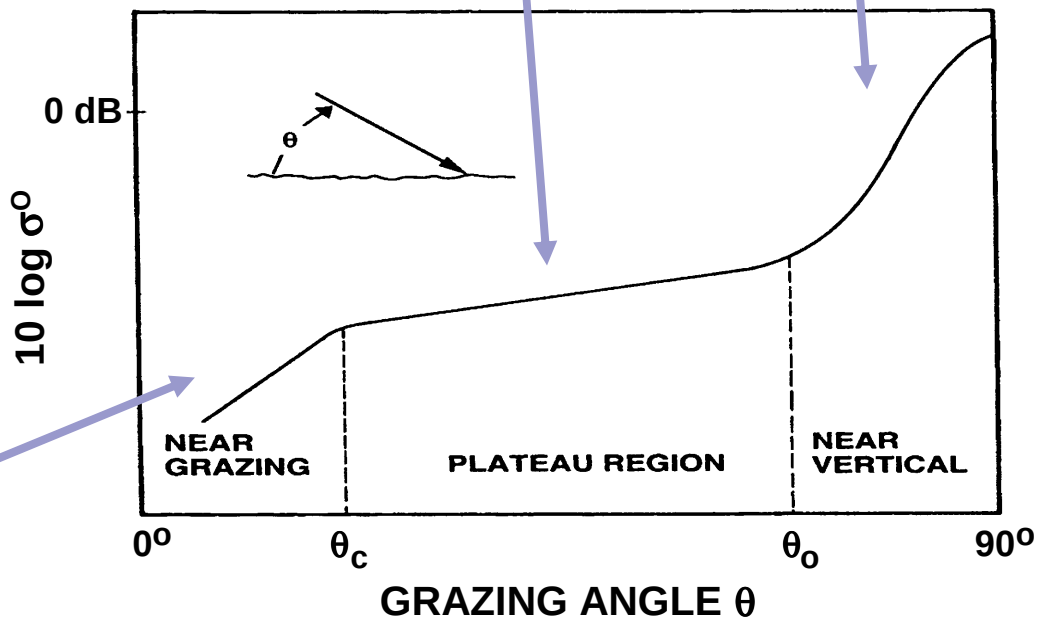

Empirical model for sea clutter σ_0

Nathanson tables [Nat69]

- The "standard" beginning 1969, updated 1990
- HH and VV POLs; 0.1°, 0.3°, 1°, 3°, 10°, 30°, 60° grazing
- Many data sources, 60 different experiments
- UHF to millimeter wavelengths
- Reported by sea state up to state 6
- Averaged without separating by wind or wave direction
- Greatest uncertainties at lower frequencies and < 3°
- Reported RCS generally larger than typical because
  (a) experimenters tend to report strongest clutter and
  (b) over-water ducting enhances apparent RCS

[Nat69] F.E. Nathanson, *Radar Design Principles*, McGraw Hill, 1969

Empirical model for sea clutter σ_0

GIT model [Hor78]

- Variables: radar wavelength, grazing angle, wind speed, wind direction from antenna boresight, wave height
- Employs separate equations: for HH and VV polarization, and for 1 to 10 GHz and 10 to 100 GHz
- The 1-10 GHz model based on data available for grazing angles of 0.1 to 10° and average wave heights up to 4 m (corresponds to significant wave heights of 6.3 m)
- Few liable $\sigma^{o}F^{4}$ data available at 3° grazing and below, and for dependencies on wind and wave directions
- Graphs from the model appear to give "best guesses" of $\sigma^{o}F^{4}$ versus grazing angles less than 10°

[Hor78] M.M. Horst, F.B. Dyer, M.T. Tuley, "Radar Sea Clutter Model", *IEEE International Conf. Antennas and Propagation*, Nov. 1978, pp 6-10.

Empirical model for sea clutter σ_0

GIT model: Wind speed dependence

- HH POL, 10 GHz
- Cross-wave direction,
  2 m signif. wave height,
  winds 3, 5, 10, 20 m/s

- $\sigma^o F^4$ increases with wind speed,
- Critical angle unchanged, because wave height assumed fixed.

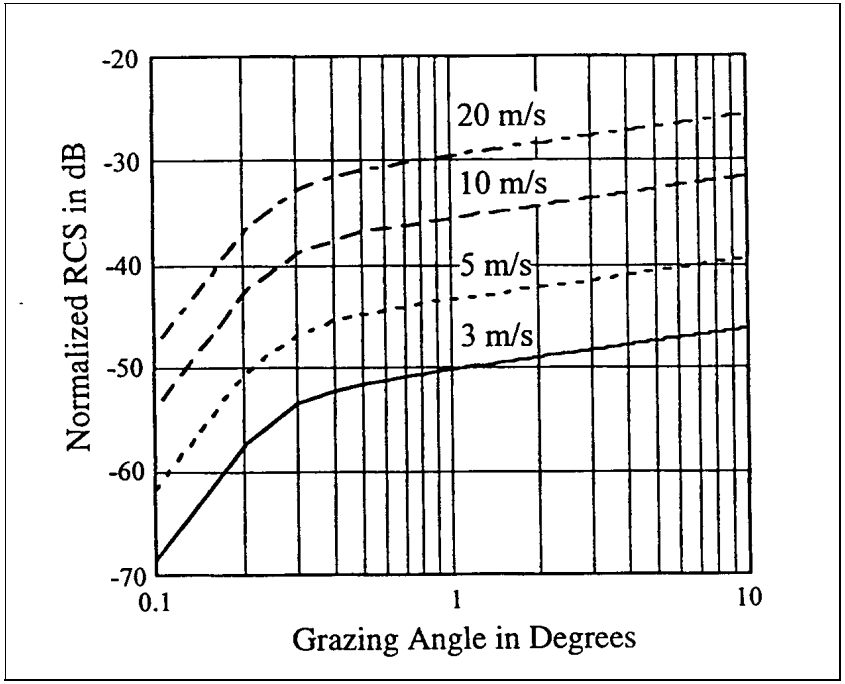

Empirical model for sea clutter σ_0

GIT model: Dependence on significant wave height $h_{1/3}$

- HH POL, 10 GHz
- Cross-wave direction,
  10 m/s wind speed,
  h1/3 = 0.5, 2, and 6 m

- In plateau region, $\sigma^o F^4$ is independent of $h_{1/3}$ (for fixed wind speed)
- $\sigma^o F^4$ increases with $h_{1/3}$ (multipath reduces critical angle) at angles < 1°

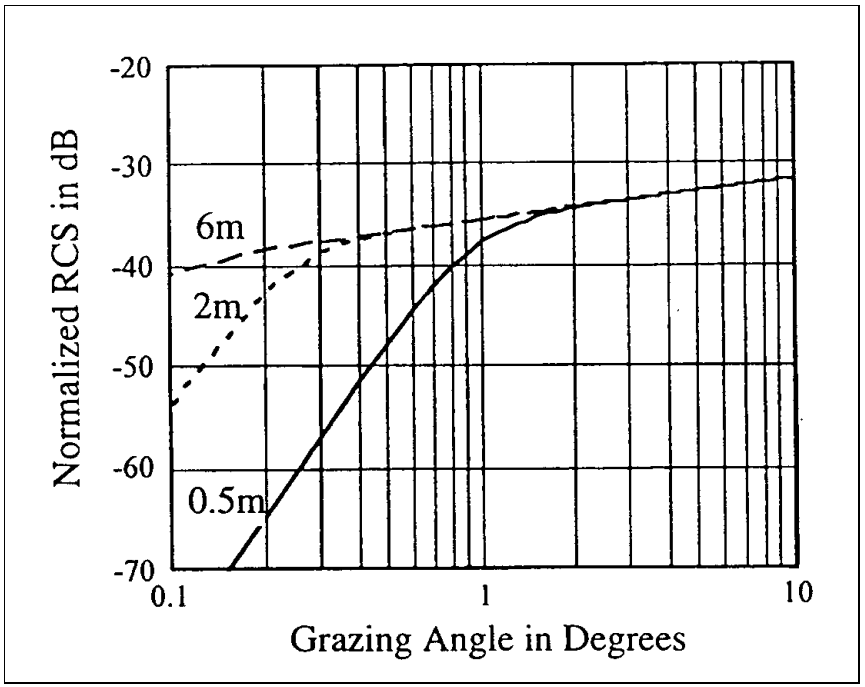

Empirical model for sea clutter σ_0

GIT model: Comparison between HH and VV POL, 10 GHz

- Wind speed/wave height in equilibrium
- $\sigma^o F^4$ increases with wind speed and $h_{1/3}$
- HH/VV ratio increases with increased surface roughness and reduced grazing angle
- HH>VV at small angles under rough conditions at 1.25 and 10 GHz

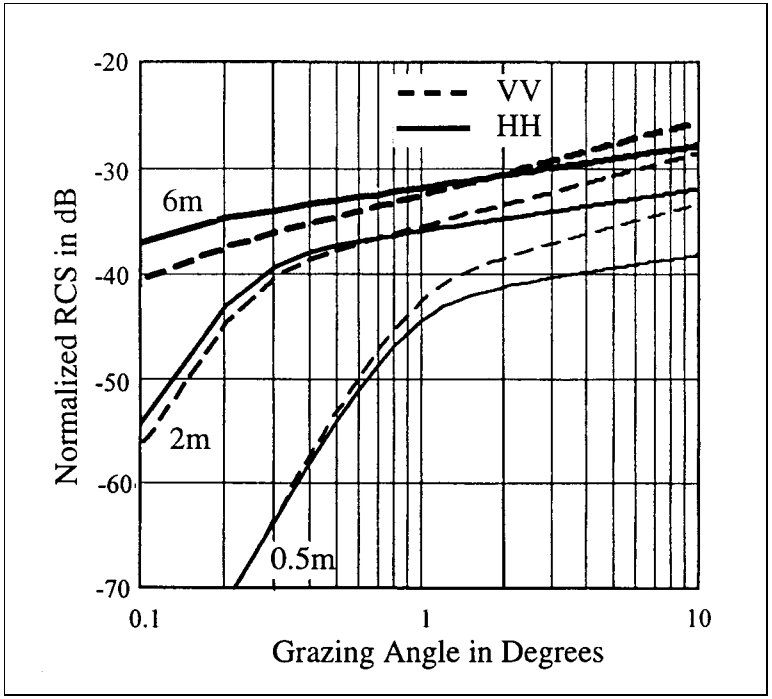

Sea clutter spikes

Bishop (1970) classified sea clutter at X-band into four types:

- Noise-like-clutter which appears similar to thermal noise with no apparent sign of periodicity;
- Clumped clutter which appears as a mixture of noise-like returns and discrete clumped clutter returns that often fades rapidly;
- Spiky clutter which consists largely of a collection of clumped returns with short persistence, e.g., 1 to 2s;
- Correlated spiky clutter consisting of persistent clumped returns. At any one time, an A-scope trace looks like a comb with semi-randomly spaced teeth. The whole pattern moves at speeds up to 40 knots. Individual spikes persisted for 10 to 40 s and the clutter level between spikes was virtually zero.

Empirical model for land clutter σ_0

σ^o vs incidence angle for rough ground [Ula89]

- 4.25 GHz data, high moisture content
- σ^o is insensitive to surface roughness at 10^o (80^o grazing)
- Same insensitivity to roughness observed at 80^o grazing in 1.1 GHz and 7.25 GHz data
- Same shapes but lower σ^o for dry conditions

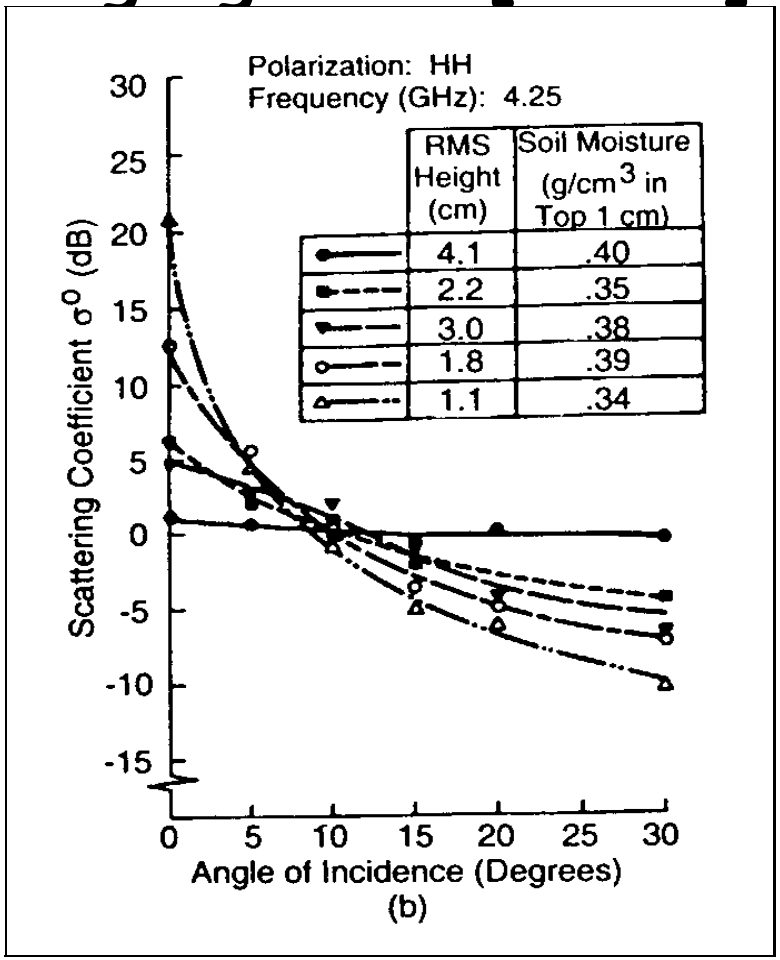

[Ula89] Ulaby, F.T. and Dobson, M.C, *Handbook of Radar Scattering Statistics for Terrain*, Artech House, Norwood MA, 1989

Land clutter σ_0 at low grazing angles

37 Rural Sites [Bil02]

- Spatial averages of $\sigma^o F^4$ for θ < 8° grazing
- Larger spreads in $\sigma^o F^4$ at lower frequencies
- Resolution 150 & 15/36 m
- HH and VV polarizations
- At each frequency, the median spatial average is roughly –30 dB
- Note: $\sigma^o F^4$ can be larger at the lower frequencies

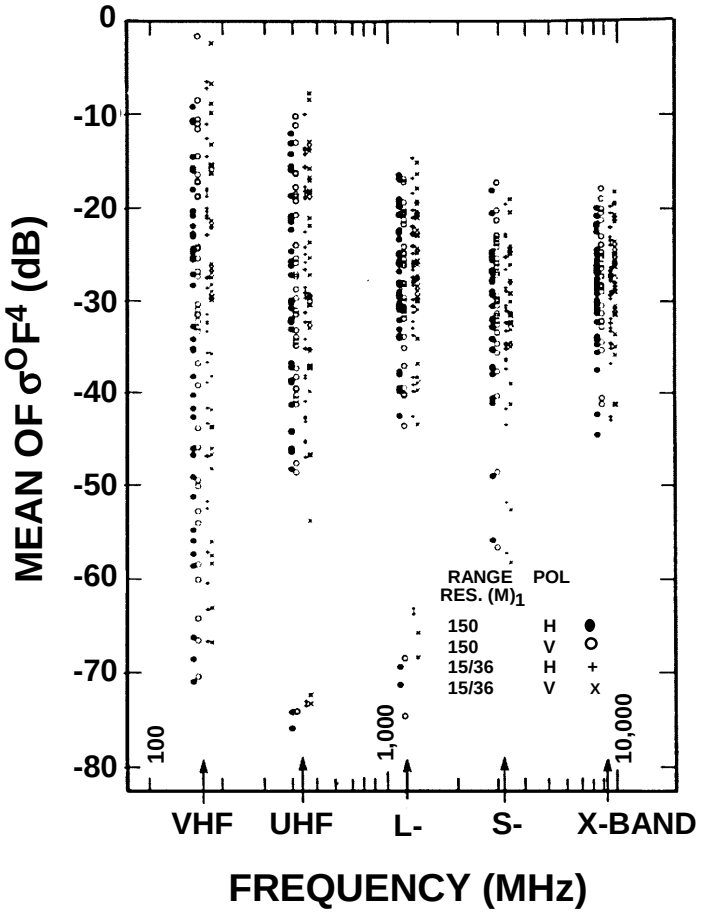

[Bil02] J.B. Billingsley, *Low-angle radar land clutter – Measurements and empirical models*, William Andrew Publishing ,Norwich, NY, 2002.

Clutter statistics: effect of spatial resolution

The scattered clutter can be written as the vector sum from N random scatterers

$$z = \sum_{\mathbf{N}} \sqrt{\sigma_{\mathbf{i}}}\, \exp[\, j\phi_i \,]$$

RCS of a single scatterer

phase term

With low resolution radars, N is deterministic and very high in each illuminated cell. Through the application of the central limit theorem (CLT) the clutter returns z can be considered as Gaussian distributed, the amplitude $r = |z|$ is Rayleigh distributed and the most important characteristic is the radar cross section.

$$p(r) = \frac{2r}{\sigma^2} \exp\left[-\frac{r^2}{\sigma^2} \right] u(r)$$

Clutter statistics: effect of spatial resolution

This is not true with high resolution systems. With reduced cell size, the number of scatterers cannot be longer considered constant but random, then improved resolution reduces the average RCS per spatial resolution cell, but it increases the standard deviation of clutter amplitude versus range and cross-range and, in the case of sea clutter, versus time as well.

Jakeman and Pusey [Jak78] showed that a modification of the CLT to include random fluctuations of the number N of scatterers can give rise to the K distribution (for amplitude PDF):

$$Z = \frac{1}{\sqrt{\bar{N}}} \sum_{i=1}^{N} a_i e^{j\varphi_i} \xrightarrow{\bar{N}\to\infty} R = |Z|$$

2-D random walk

K distributed if N is a negative binomial r.v. (Gaussian distributed if N is deterministic, Poisson, or binomial)

$$\bar{N} = E\{N\}, \{a_i\}\ i.i.d., \{\varphi_i\}\ i.i.d.$$

The compound-Gaussian model

In general, taking into account the variability of the local power τ, that becomes itself a random variable, we obtain the so-called compound-Gaussian model, then

$$p(r \mid \tau) = \frac{2r}{\tau} \exp\left[-\frac{r^2}{\tau}\right] u(r)$$

$$p(r) = \int_0^\infty p(r \mid \tau)\ p(\tau)\ d\tau; \quad 0 \le r \le \infty$$

According to the CG model:

$$z(n) = \sqrt{\tau(n)}\, x(n)$$

$$x(n) = x_I(n) + j x_Q(n)$$

Texture: non negative random process, takes into account the local mean power

Speckle: complex Gaussian process, takes into account the local backscattering

The compound-Gaussian model

Particular cases of CG model (amplitude PDF):

K (Gamma texture) ⇨

$$p_R(r) = \frac{\sqrt{4\nu/\mu}}{2^{\nu-1}\Gamma(\nu)}\left(\sqrt{\frac{4\nu}{\mu}}r\right)^{\nu} K_{\nu-1}\left(\sqrt{\frac{4\nu}{\mu}}r\right)u(r)$$

GK (Generalized Gamma texture) ⇨

$$p_R(r) = \frac{2br}{\Gamma(\nu)}\left(\frac{\nu}{\mu}\right)^{\nu b}\int_0^{\infty}\tau^{\nu b-2}\exp\left[-\frac{r^2}{\tau}-\left(\frac{\nu}{\mu}\tau\right)^{b}\right]d\tau$$

LNT (log-normal texture) ⇨

$$p_R(r) = \frac{r}{\sqrt{2\pi\sigma^2}}\int_0^{\infty}\frac{2}{\tau^2}\exp\left[-\frac{r^2}{\tau}-\frac{1}{2\sigma^2}\left[\ln(\tau/\delta)\right]^2\right]d\tau$$

W, Weibull ⇨

$$p_R(r) = \frac{c}{b}\left(\frac{r}{b}\right)^{c-1}\exp\left[-(r/b)^{c}\right]u(r)$$

The K model

K-PDF (amplitude PDF)

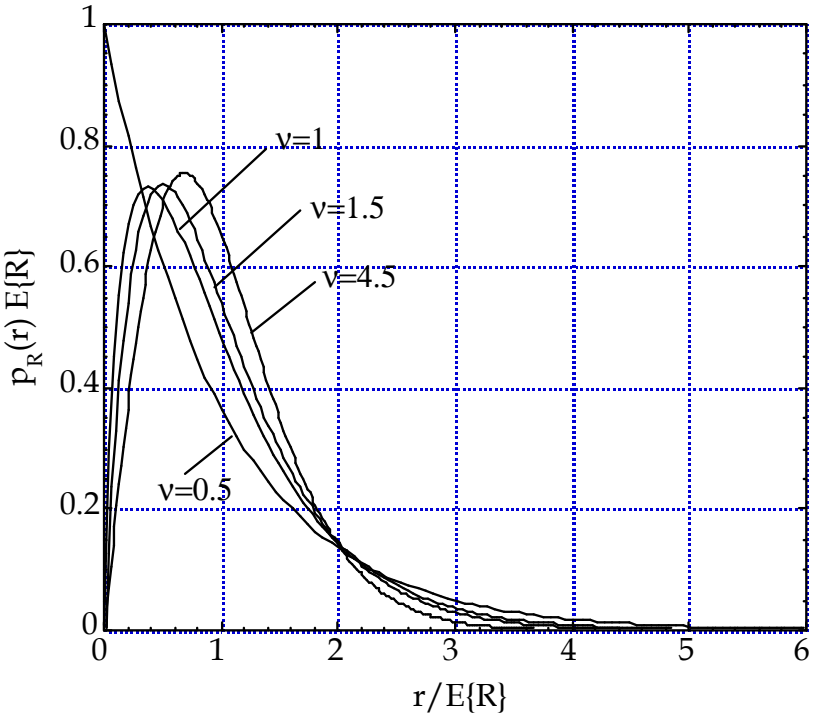

- The order parameter ν is a measure of clutter spikiness
- The clutter becomes spikier as ν decreases
- Gaussian clutter: $\nu \to \infty$

The K model is a special case of the compound-Gaussian model:
N = negative binomial r.v.
τ (local clutter power) = Gamma distributed
Amplitude R = K distributed

Gamma-PDF (texture PDF)

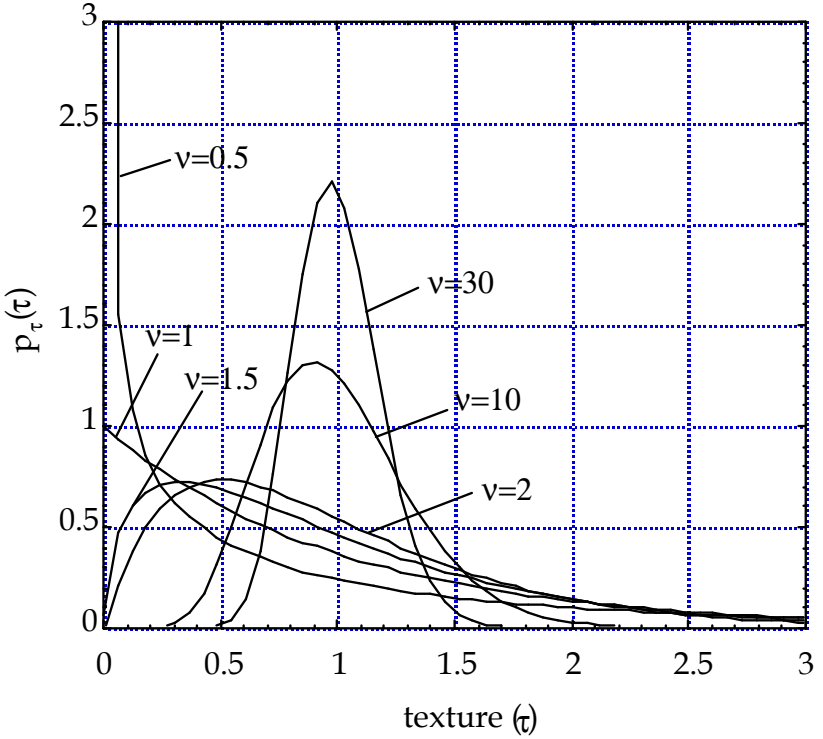

The multidimensional compound-Gaussian model

• In practice, radars process *M* pulses at time, thus, to determine the optimal radar processor we need the *M*-dimensional joint PDF
• Since radar clutter is generally highly correlated, the joint PDF cannot be derived by simply taking the product of the marginal PDFs
• The appropriate multidimensional non-Gaussian model for use in radar detection studies must incorporate the following features:

1) it must account for the measured first-order statistics (i.e., the APDF should fit the experimental data)

2) it must incorporate pulse-to-pulse correlation between data samples

3) it must be chosen according to some criterion that clearly distinguishes it from the multitude of multidimensional non-Gaussian models, satisfying 1) and 2)

The multidimensional compound-Gaussian model

• If the Time-on-Target (ToT) is short, we can consider the texture as constant for the entire ToT, then the compound-Gaussian model degenerates into the spherically invariant random process (SIRP) proposed by Conte and Longo [Con87] for modeling the radar sea clutter. By sampling a SIRP we obtain a spherically invariant random vector (SIRV) whose PDF is given by

$$p_Z(\mathbf{z}) = \int_0^\infty \frac{1}{(\pi\tau)^M |\mathbf{M}|} \exp\left(-\frac{\mathbf{z}^H \mathbf{M}^{-1} \mathbf{z}}{\tau}\right) p_\tau(\tau)\, d\tau$$

where $\mathbf{z}=[z_1\ z_2 \ldots z_M]^T$ is the M-dimensional complex vector representing the observed data.

• A random process that gives rise to such a multidimensional PDF can be physically interpreted in terms of a locally Gaussian process whose power level τ is random.

• The PDF of the local power τ is determined by the fluctuation model of the number N of scatterers.

Sea and land clutter APDFs

First order statistics:

The homogeneity of sea allows to consider its spatial distribution equivalent to the temporal distribution. The same is not true for land clutter. The most common distributions for the sea clutter are the K, GK and Weibull.

Because of the large spatial variability of land clutter the statistics in space and time are different. The most common are in the table below.

	1st order
Time	Rayleigh, Rice, Weibull, Log-normal
Space	Weibull, Log-normal

Power Spectral Density (PSD) models

- The question is: **How to specify the clutter covariance matrix and the power spectral density?**

- Correct spectral shape impacts clutter cancellation and target detection performance.
- The clutter spectrum is not concentrated at zero Doppler only, but spreads at higher frequencies.
- There are several reasons for the clutter spreading:
  - Wind-induced variations of the clutter reflectivity (sea waves, windblown vegetations, etc.).
  - Amplitude modulation by the mechanically scanning antenna beam.
  - Pulse-to-pulse instabilities of the radar system components.
  - Transmitted frequency drift.
- The pulse-to-pulse fluctuation is generally referred to as internal clutter motion (ICM).

PSD models

The PSD is often modeled as having a Gaussian shape:

$$S_G(f) = S_{0G} \exp\left[-\frac{\left(f - m_f\right)^2}{2\sigma_f^2} \right]$$

This is usually a mathematical convenience rather than any attempt at realism. Often the Doppler spectrum will be strongly asymmetric and the mean Doppler shift, m_f, may not be zero. Clearly for land clutter m_f is usually zero, but for rain and sea clutter in general $m_f \neq 0$ and will be dependent on the wind speed and direction.

From velocity/Doppler relationship $v = f_D\lambda/2$,
standard dev. of scatterer velocity is $\sigma_v = \sigma_f\lambda/2$
Wind changes bandwidths, but typical σ_v are

Rain/chaff σ_v~1 to 2 m/s
Sea σ_v~1 m/s
Land σ_v~0 to 0.5 m/s

PSD models: windblown ground clutter

The Gaussian PSD model was proposed by Barlow [Bar49] for **windblown clutter spectra**, for noncoherent radar systems and over limited spectral dynamic ranges (up to a level 20 dB below the peak level and to a maximum Doppler velocity of 0.67 m/s)

Essentially all modern measurements of ground clutter spectra, with increased sensitivity compared to those of Barlow, without exception show spectral shapes wider than Barlow's Gaussian in their tails

It had become theoretically well understood from 1965-67 on, that branch motion in windblown vegetation generates spectra wider than Gaussian

In a much referenced later report, Fishbein et al. [Fis67] introduced the power-law clutter spectral shape:

$$P_{ac}(f) = \frac{n\sin(\pi/n)}{2\pi f_c} \frac{1}{1+(f/f_c)^n}$$

f_c: break-point Doppler frequency where the shape function is 3 dB below its peak zero-Doppler level

n: n is the shape parameter

PSD models: windblown ground clutter

Common values of power-law exponent *n* used in PSD modeling are usually on the order of 3 or 4, but sometimes greater
The evidence that clutter spectra have power-law shapes over spectral dynamic ranges reaching 30 to 40 dB below zero-Doppler peaks is essentially empirical, not theoretical.

However, there is no simple physical model or fundamental underlying reason requiring clutter spectral shapes to be power law.

Recently, **Billingsley** [Bil91] showed that measurements at MIT-LL of windblown ground clutter power spectra to levels substantially lower than most earlier measurements (i.e., 60 to 80 dB below zero-Doppler peaks) indicate spectral shapes that fall off much more rapidly than constant power-law at the lower levels, at rates of decay approaching **exponential**:

$$P_{ac}(f) = \frac{\lambda\beta_e}{4}\exp\left(-\frac{\lambda\beta_e}{2}|f|\right)$$

λ is the radar transmission wavelength and β_e is the exponential shape parameter

PSD models: windblown ground clutter

Then, recent studies have demonstrated that the ground clutter spectrum of windblown trees consists of three components:

- coherent component
- slow diffuse component
- fast-diffuse component

The *coherent component* was the results of radar returns from steady objects such as buildings, highways and from movable objects at rest.

The coherent component is at zero Doppler.

Slow-diffuse & fast-diffuse components

The *slow-diffuse component* is the consequence of motions of objects with moderate inertia (tree branches).

The slow-diffuse component occupies a relative narrow region around zero Doppler.

The spectrum is approximately symmetrical and its spectral density in dB scale decreases linearly with increasing absolute values of Doppler frequency.

The *fast-diffuse component* is the result of movements in light objects such as a tree leaves. This component has a spectral density similar to a band-limited noise. Its magnitude is usually compared to other components.

The spectral extent is of the same order as the Doppler shifts that corresponds to the wind speed.

PSD models: windblown ground clutter

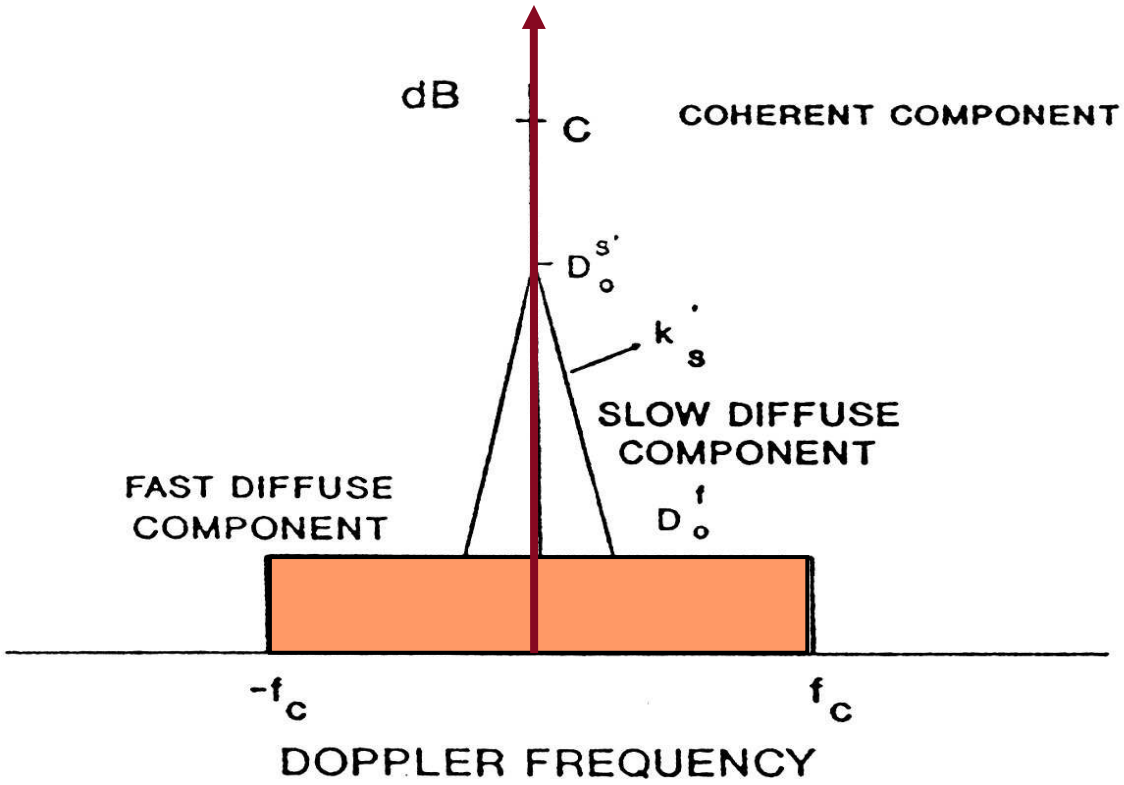

Symbolic diagram of a ground-clutter spectral model.

PSD models: windblown ground clutter

Spectral shapes having equal AC (Fluctuating) Power
- Source: Billingsley (1996)

- Each spectrum for wind speed of about 20 mph
- The Gaussian shape reported by Barlow (1949)
- The power-law shape from Fishbein et al. (1967)
- The exponential shape from Billingsley and Larrabee (1987)

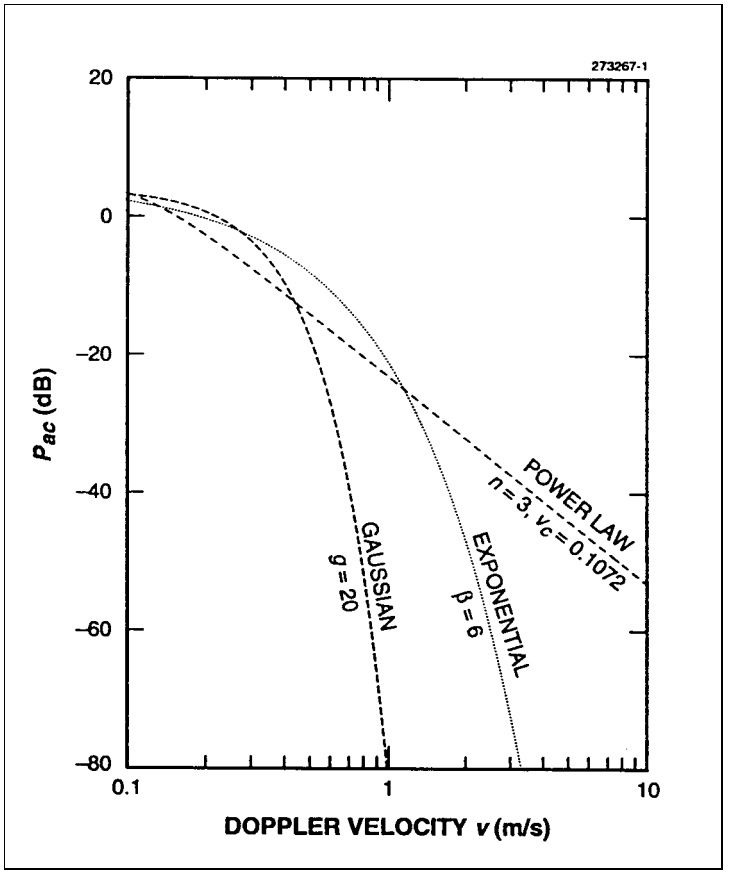

Ground clutter spectra: X-band

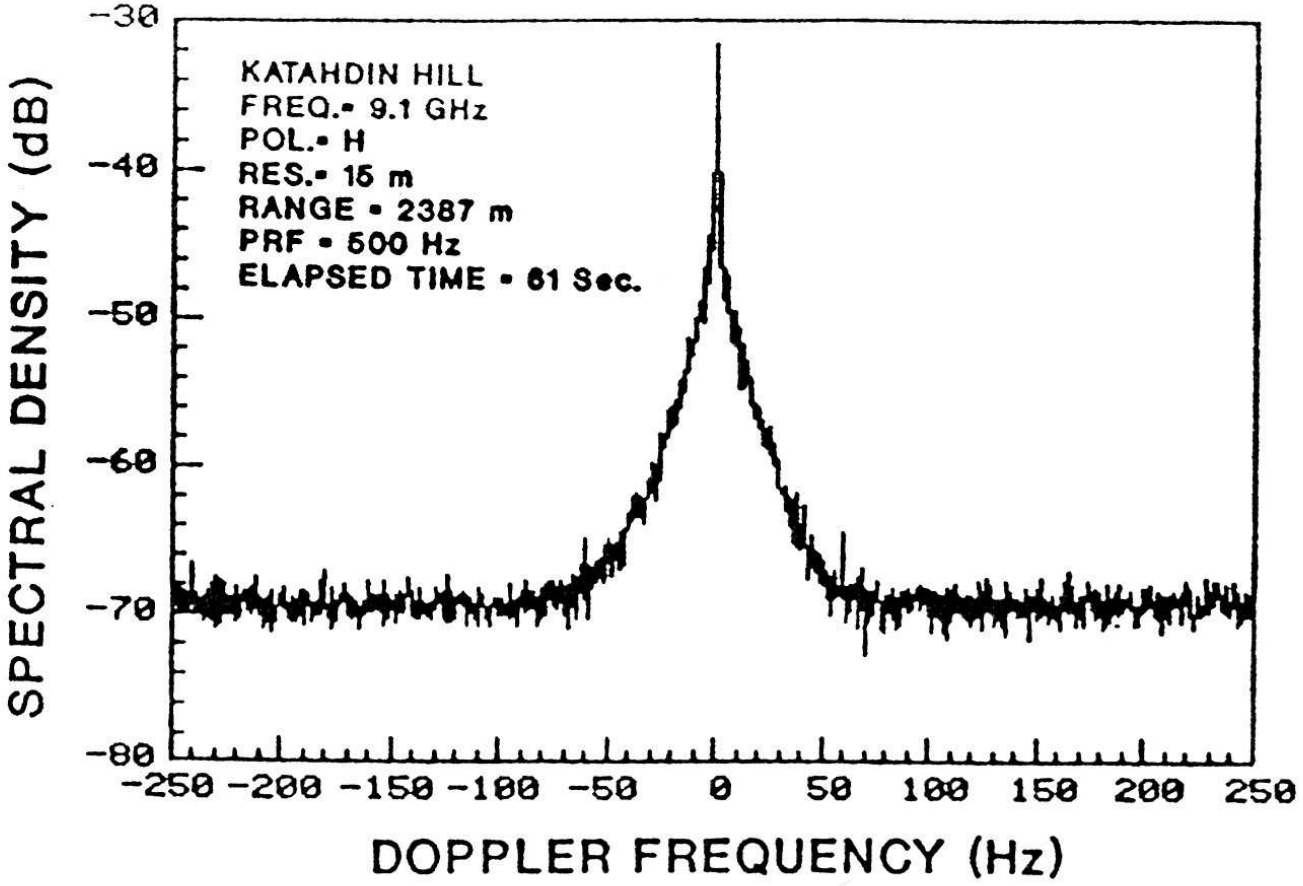

A typical X-band ground-clutter spectrum.

Ground clutter spectra: S-band

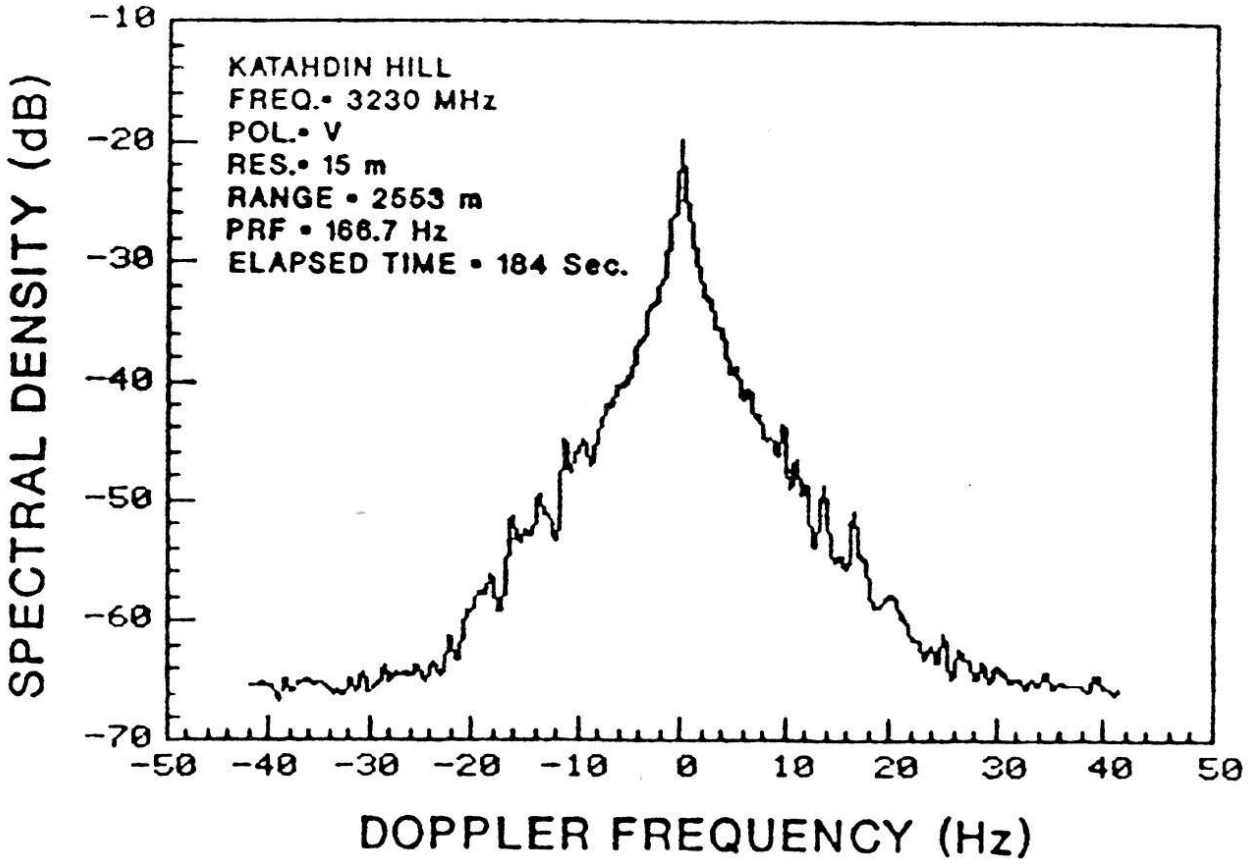

A typical S-band ground-clutter spectrum.

Variation of the spectral slope diffuse components

S-band

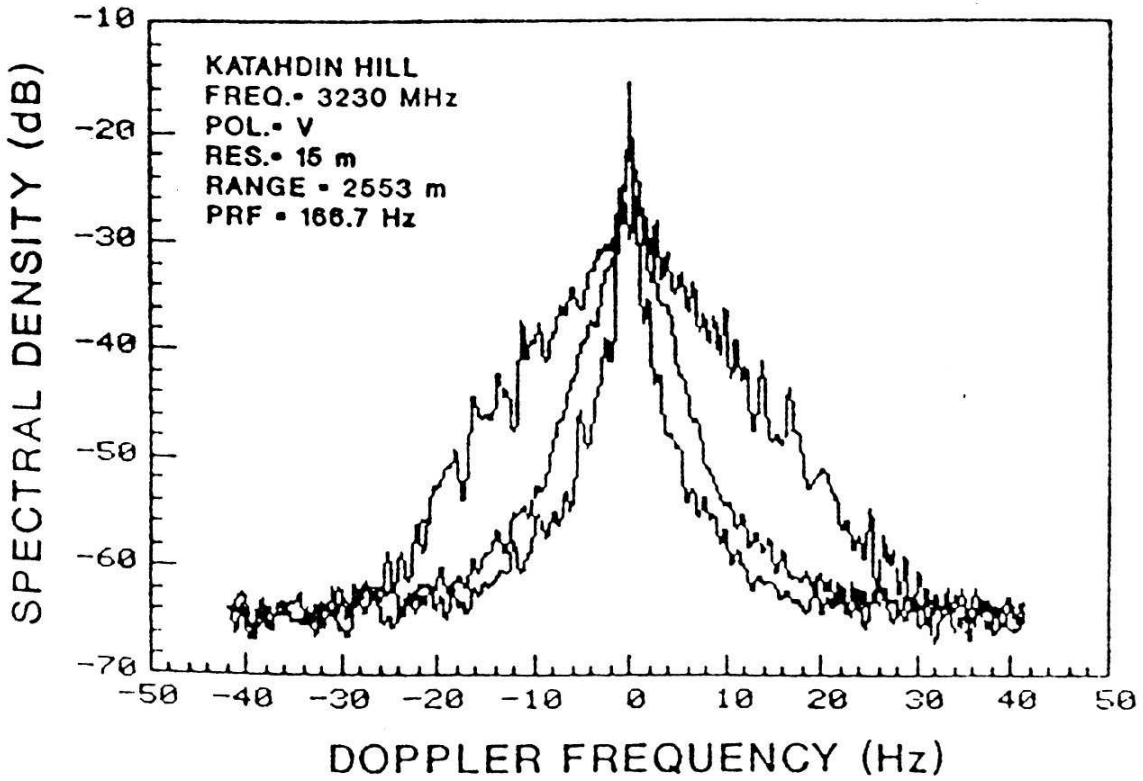

Variation of the spectral slope of the slow diffuse component over an observation interval.

L-Band forest PSD vs wind speed

- Approximate linear dependence of power density in dB versus velocity, for all wind speeds
- For VHF through X band, measured spectral shapes versus Doppler velocity found to be essentially the same

Source: Billingsley (1996).

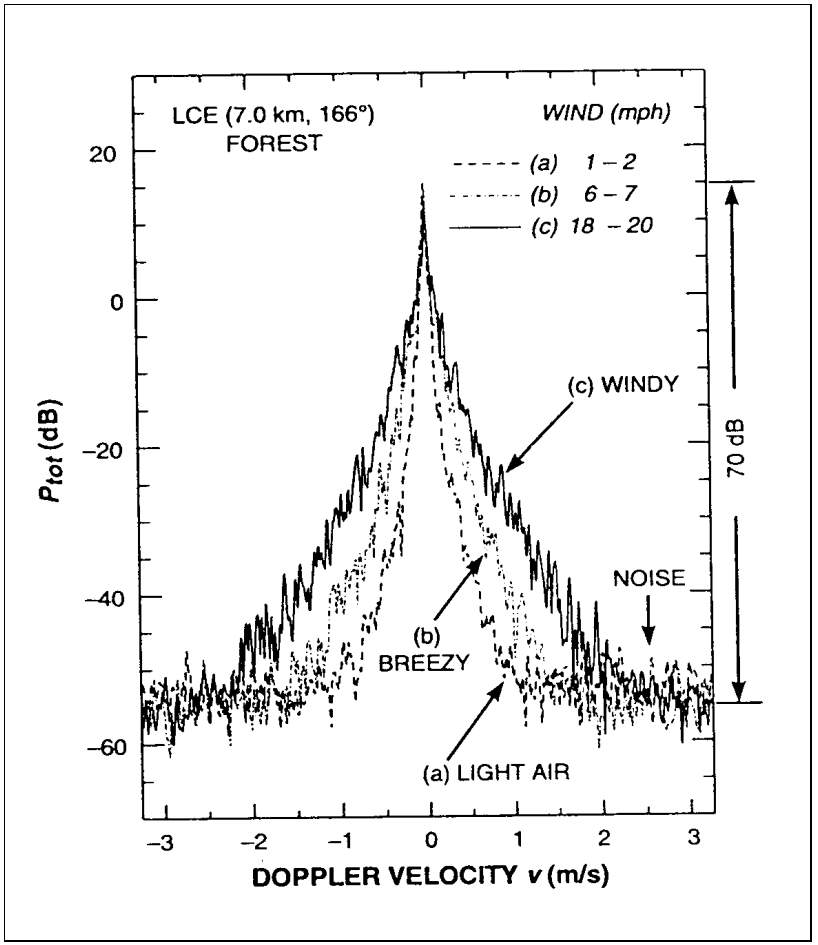

Sea clutter PSD

The relative motion of the sea surface with respect to the radar causes an intrinsic Doppler shift of the return from individual scatterers.

Because the motion of the scattering elements have varying directions and speeds the total echo contains a spectrum of Doppler frequencies.

Two effects are of interest:

- the spectral shape and width
- the mean Doppler shift of the entire spectrum.

Sea clutter PSD

The spectrum of sea clutter is sometimes assumed to have Gaussian shape. An approximate relationship between the -3dB bandwidth Δf of the spectrum and sea state S (Douglas scale) has been derived by Nathanson:

$$\Delta f = 3.6\, f_{0(GHz)} S$$

The standard deviation of the Gaussian spectrum is related to Δf by the expression:

$$\sigma_f = 0.42 \Delta f$$

Recently more complex and realistic models have been proposed for sea clutter PSD. We are going to analyze them later on.

Radar Clutter: Live recorded data

IPIX Radar Description

Transmitter

- frequency agility (16 frequencies, X-band)
- H and V polarizations, switchable pulse-to-pulse
- pulse width 20 ns to 5000 ns
- PRF=0 to 20 KHz

Receiver

- coherent receiver
- 2 linear receivers; H or V on each receiver
- quantization: 8 to 10 bits
- sample rate: 0 to 50 MHz
- BW=5.5 MHz

Antenna

- parabolic dish (2.4 m)
- pencil beam (beamwidth 1.1°)
- grazing angle <1°, fixed or scanning

Source: Defense Research Establishment Ottawa.

Sea clutter temporal behaviour (30 m)

The spikes have different behaviour in the two like-polarizations (HH and VV)

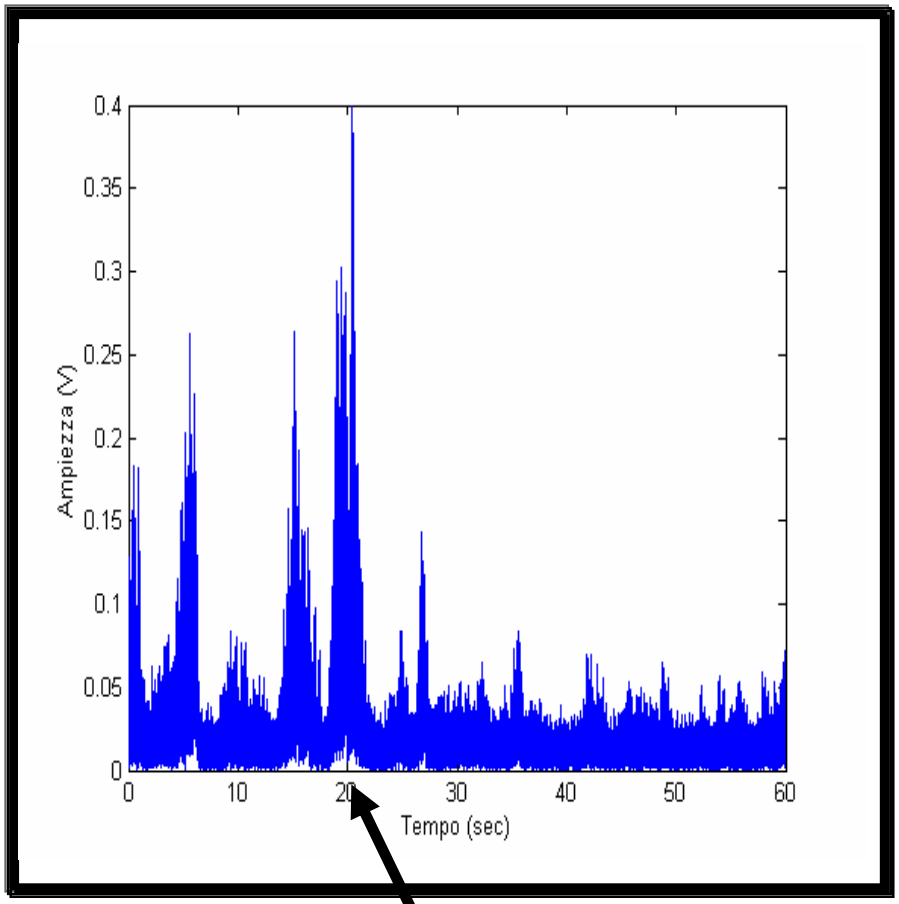

The dominant spikes on the HH record persist for about 1-3 s.

The vertically polarized returns appear to be a bit broader but less spiky

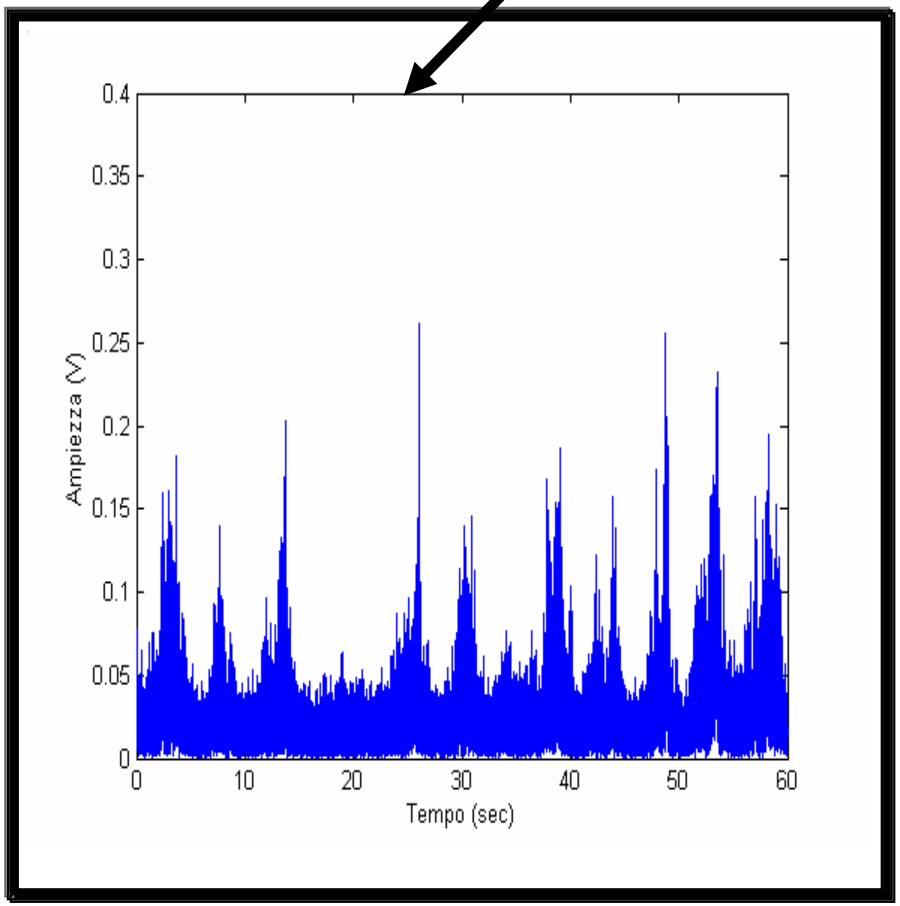

Sea clutter

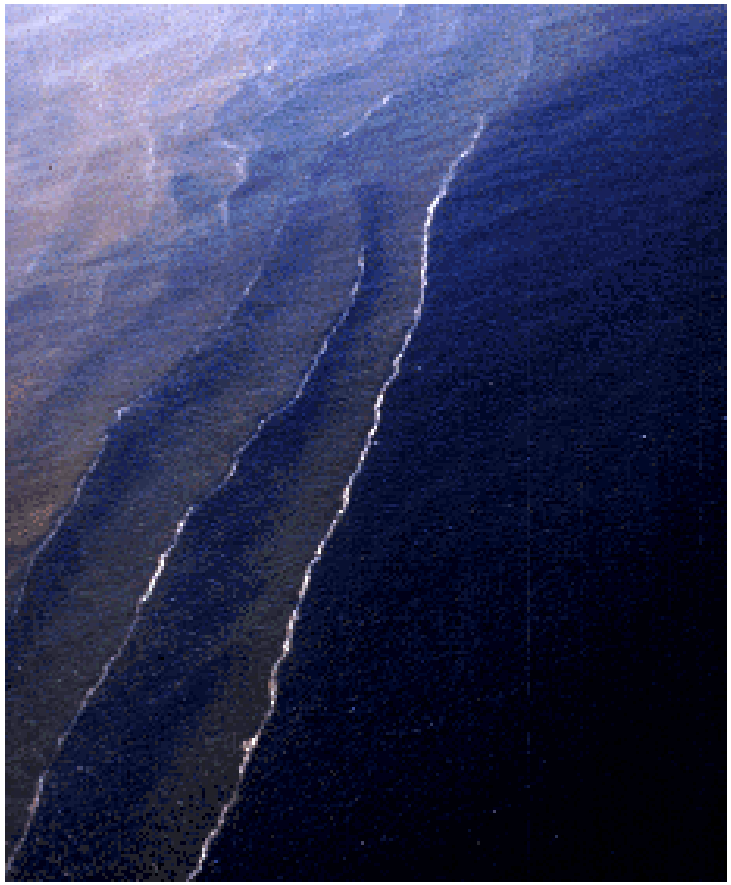

Long waves or swells

Waves and whitecaps

Sea clutter temporal behaviour (30 m)

Waves 80 cm high

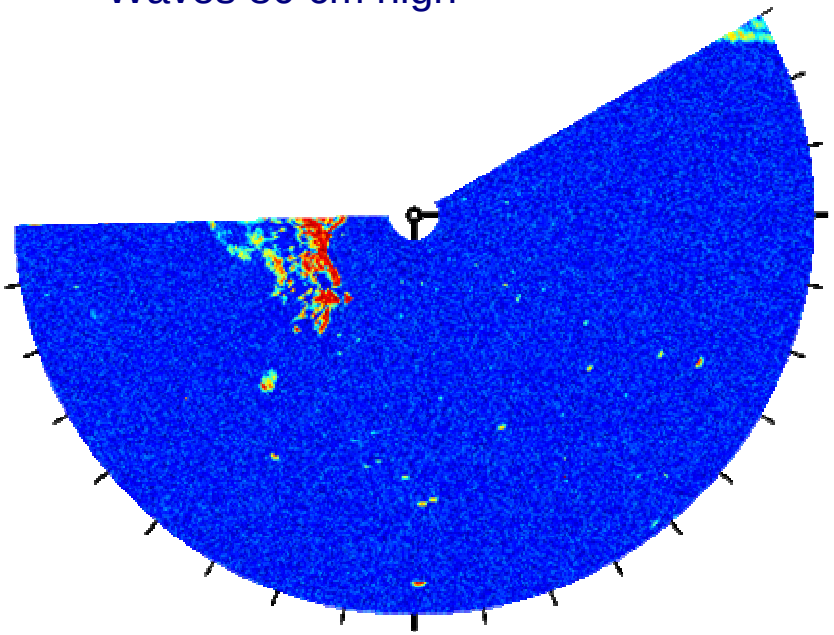

IPIX radar

Waves 2.4 m high

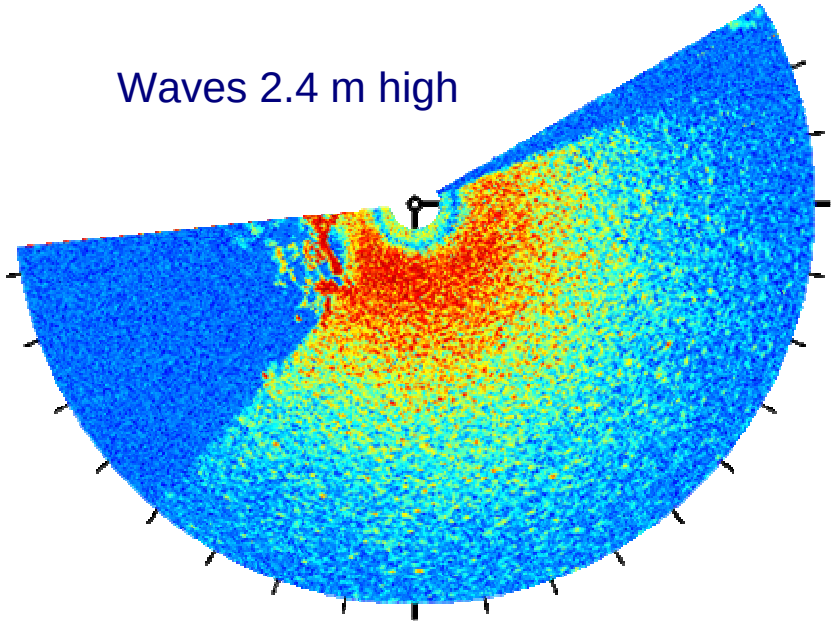

McMaster University

Inspiring Innovation and Discovery

Data Description

Dataset	19980204_223753	19980204_220849	19980204_223220	19980204_224024	19980204_223506
Date and time	02/04/1998 22:37:53	02/04/1998 22:08:49	02/04/1998 22:32:20	02/04/1998 22:40:24	02/04/1998 22:35:06
# Range cells	28	28	28	28	27
Start range	3201 m	3201 m	3201 m	3201 m	3201 m
Range res.	60 m	30 m	15 m	9 m	3 m
Pulse width	400 ns	200 ns	100 ns	60 ns	20 ns
# Sweep	60000	60000	60000	60000	60000
Sample per cell	60000	60000	60000	60000	60000
PRF	1 KHz	1 KHz	1 KHz	1 KHz	1 KHz
RF-freq.	9.39 GHz	9.39 GHz	9.39 GHz	9.39 GHz	9.39 GHz
Radar and wave geometry	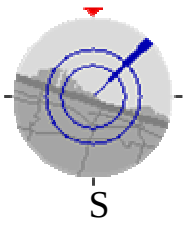	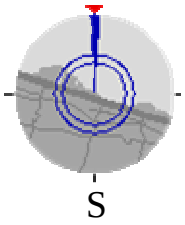	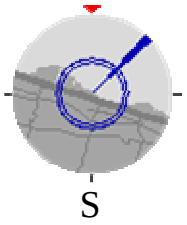	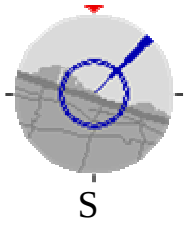	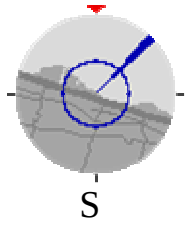

Statistical Analysis: Amplitude Models

LN, log-normal

$$p_R(r) = \frac{1}{r\sqrt{2\pi\sigma^2}} \exp\left(-\frac{1}{2\sigma^2} \left[\ln(r/\delta) \right]^2 \right) u(r)$$

W, Weibull

$$p_R(r) = \frac{c}{b} \left(\frac{r}{b} \right)^{c-1} \exp\left[-(r/b)^c \right] u(r)$$

K (Gamma texture)

$$p_R(r) = \frac{\sqrt{4\nu/\mu}}{2^{\nu-1}\Gamma(\nu)} \left(\sqrt{\frac{4\nu}{\mu}} r \right)^{\nu} K_{\nu-1}\left(\sqrt{\frac{4\nu}{\mu}} r \right) u(r)$$

GK (Generalized Gamma texture)

$$p_R(r) = \frac{2br}{\Gamma(\nu)} \left(\frac{\nu}{\mu} \right)^{\nu b} \int_0^{\infty} \tau^{\nu b - 2} \exp\left[-\frac{r^2}{\tau} - \left(\frac{\nu}{\mu} \tau \right)^b \right] d\tau$$

LNT (log-normal texture)

$$p_R(r) = \frac{r}{\sqrt{2\pi\sigma^2}} \int_0^{\infty} \frac{2}{\tau^2} \exp\left[-\frac{r^2}{\tau} - \frac{1}{2\sigma^2} \left[\ln(\tau/\delta) \right]^2 \right] d\tau$$

Histogram and moments

•A histogram is a graphical representation used to plot density of data, and often for density estimation.

•A histogram consists of tabular frequencies, shown as adjacent rectangles, erected over discrete intervals (bins), with an area equal to the frequency of the observations in the interval. The height of a rectangle is also equal to the frequency density of the interval, i.e., the frequency divided by the width of the interval. The total area of the histogram is equal to the number of data.

•A histogram may also be normalized displaying relative frequencies. In that case the total area is 1. The bins must be adjacent, and often are chosen to be of the same size.

Statistical Analysis: Results - 15 m

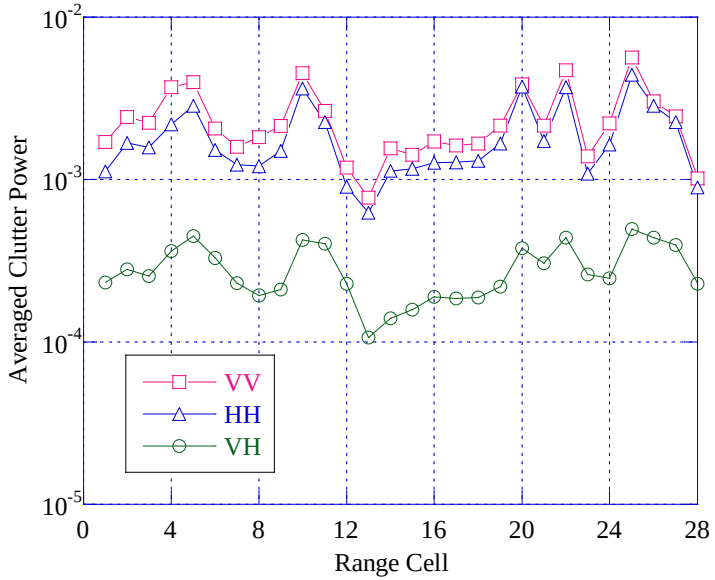

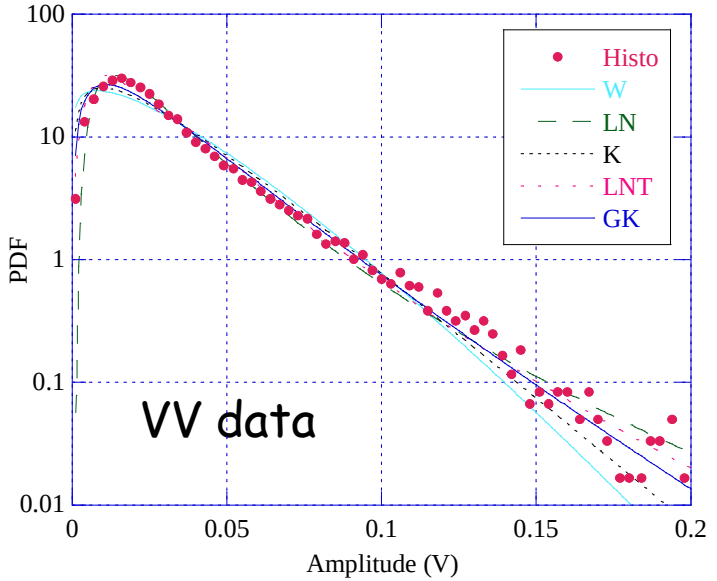

- With resolution of 60 m, 30 m, and 15 m a very good fitting with the GK-PDF.
- Negligible differences among polarizations

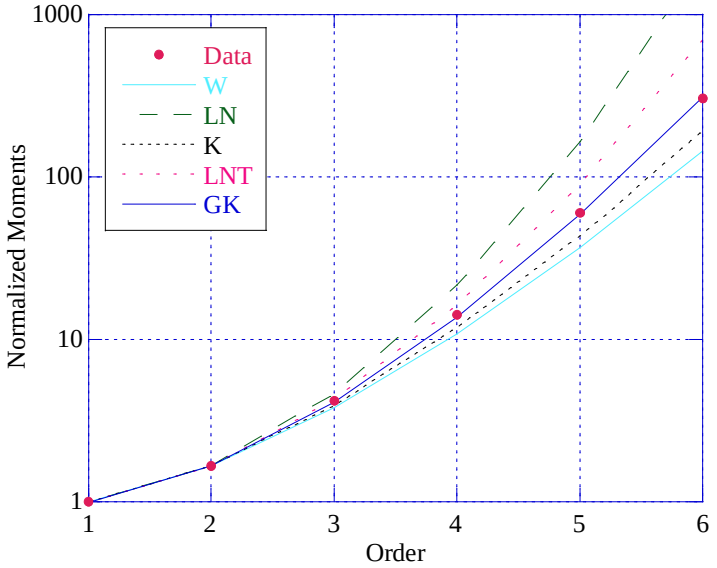

Statistical Analysis: Results - 3 m

- With resolution of 9 m and 3 m histograms with very long tails
- Not big differences among polarizations, but generally HH data spikier than VV data

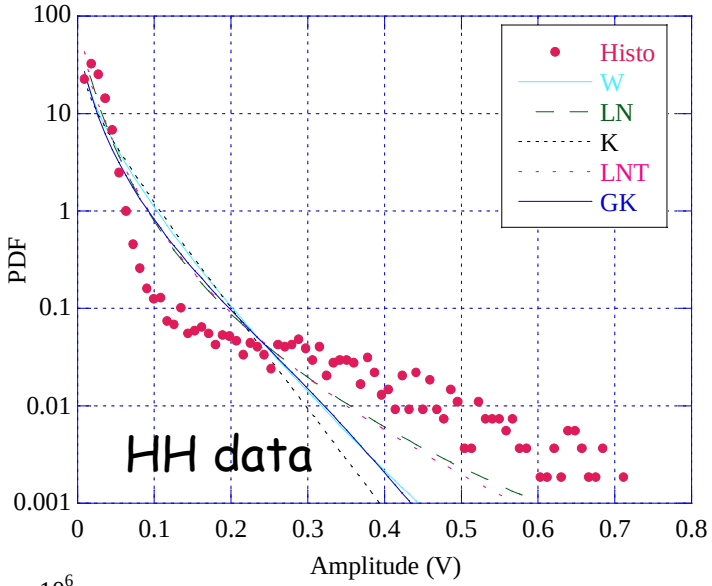

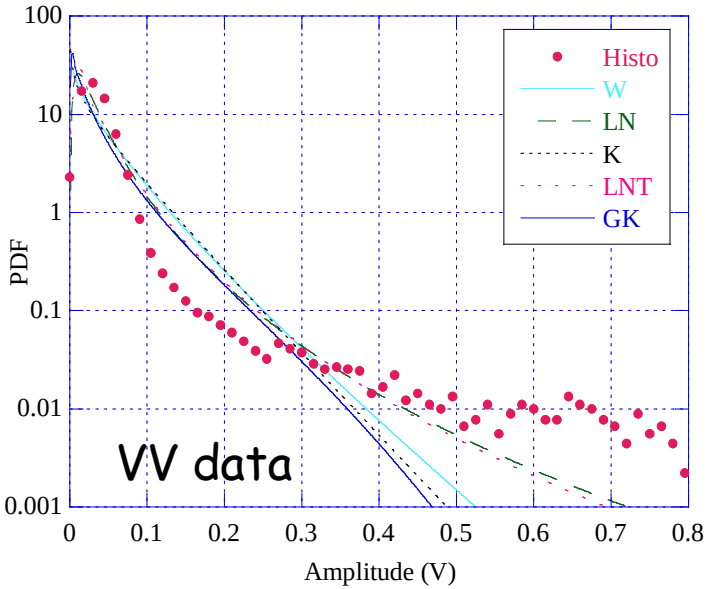

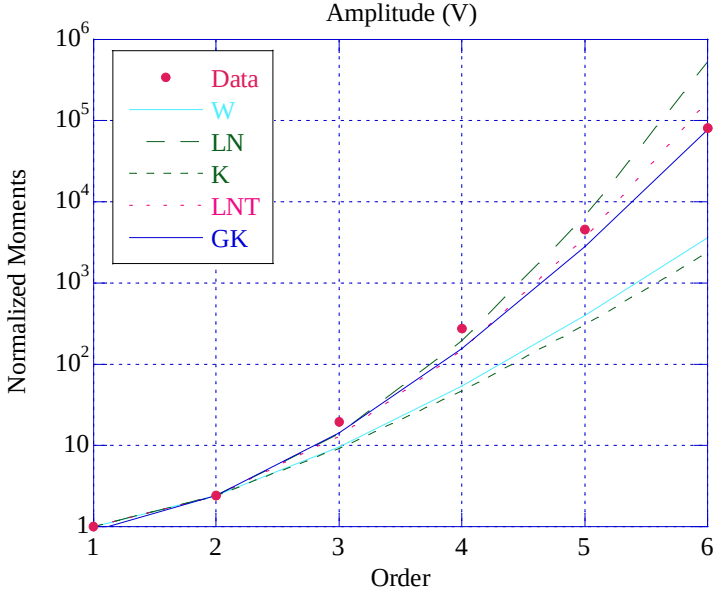

Average spectral models

Sea clutter average spectra

✓ Capillary waves with wavelengths on the order of centimetres or less. Generated by turbulent gusts of near surface wind; their restoring force is the surface tension.

✓ Longer gravity waves (sea or swell) with wavelengths ranging from a few hundred meters to less than a meter. Swells are produced by stable winds and their restoring force is the force of gravity.

Sea clutter average spectra

- In the literature, it has been often assumed that the sea clutter has **Lorentzian** spectrum (i.e., autoregressive of order 1).

- **Autoregressive (AR)** models with the order *P* ranging from 2 to 5 have also been proposed for modelling radar clutter.

- For the sea surfaces some experimental analysis at small grazing angle, C and X-bands, indicate that the sea Doppler spectrum cannot be expressed by the Bragg mechanism only, but also by wave bunching (**super-events**).

Sea clutter average spectra

- Lee *et al.* showed that the spectral lineshapes can be decomposed into three **basis functions** which are **Lorentzian**, **Gaussian**, and **Voigtian** (convolution of the Gaussian and Lorentzian):

$$S(f) = \frac{\Gamma/2\pi^2}{(f - f_L)^2 + (\Gamma/2\pi)^2}$$

peak of the Lorentzian function

Γ^{-1} = characteristic scatterer lifetime

$$S(f) = \frac{a}{\pi} \int_{-\infty}^{\infty} \frac{\exp(-x^2)}{\left(\frac{f - f_V}{f_{Ve}} - x\right) + a^2} dx$$

$a = \Gamma/2\pi f_{Ve}$ shape parameter

f_V = centre of the Voigt function

How to estimate the clutter PSD

- The PSD can be estimated parametrically (or model-based) or non-parametrically, without any hypothesis on the model.

- Non parametrically, we used the periodogram defined as:

$$P(f) = \frac{|Z(f)|^2}{M}$$

  - where $Z(f)$ is the Fourier Transform of the data and *M* the number of samples.

- There are many variants of the periodogram (for instance, method of Welch, Blackman and Tukey) [see e.g. Stoica and Moses book on Power Spectral Analysis].

Sea clutter average spectra

The spectrum is the sum of two basis functions among: the Gaussian, the Lorentzian, and the Voigtian, with different Doppler peaks.

non-par: periodogram
Gauss and Voigtian basis functions

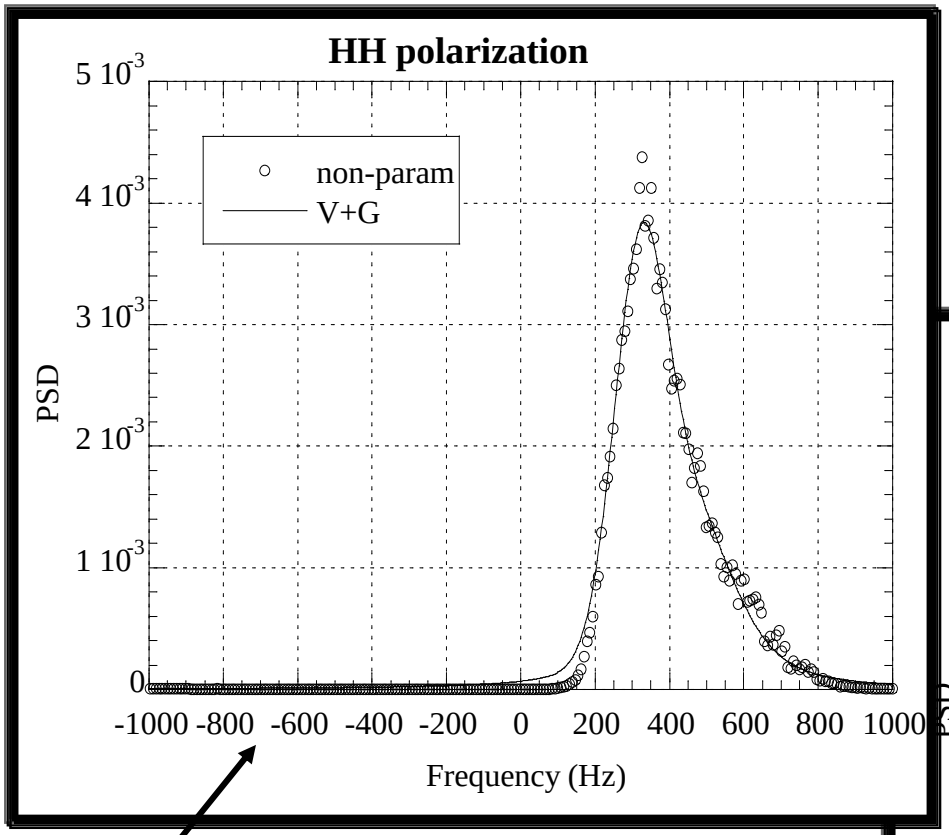

High peak (Voigtian): 450 Hz
Low peak (Gaussian): 320 Hz

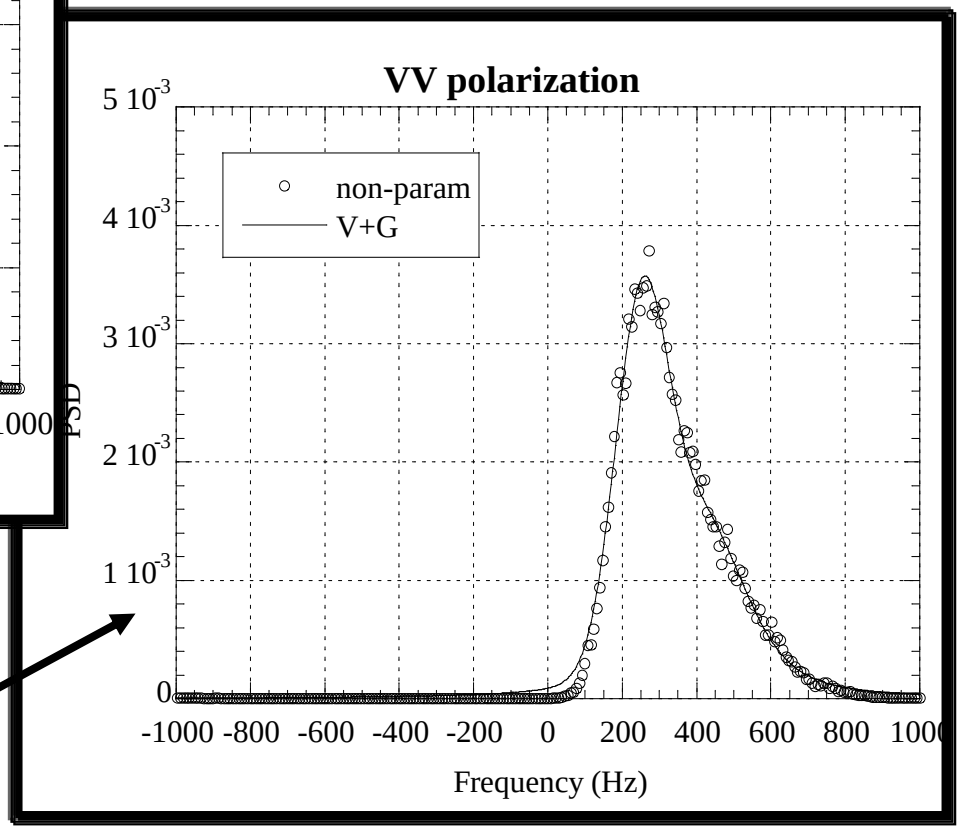

High peak (Voigtian): 410 Hz
Low peak: (Gaussian): 250 Hz

AR modelling

- An Autoregressive process of order P, AR(*P*), is characterized by the difference equation:

$$Z(n) = \sum_{k=1}^{P} a_{P,k} Z(n-k) + W(n)$$

where the coefficients $a_{P,k}$ are the process parameters, and *W*(*n*) is white noise

- For estimating the AR(P) parameters, we use the Yule-Walker equations

$$\begin{bmatrix} R_z(0) & R_z(1) & \cdots & R_z(P-1) \\ R_z(-1) & R_z(0) & & \vdots \\ \vdots & & \ddots & R_z(1) \\ R_z(1-P) & \cdots & R_z(-1) & R_z(0) \end{bmatrix} \begin{bmatrix} a_{P,1} \\ a_{P,2} \\ \vdots \\ a_{P,P} \end{bmatrix} = \begin{bmatrix} R_z(1) \\ R_z(2) \\ \vdots \\ R_z(P) \end{bmatrix}$$

$$\mathbf{Ra} = \mathbf{r}$$

- In our case, we don't know the "true" correlation of the clutter, so we estimate it as

$$\hat{R}_Z(m) = \frac{1}{N} \sum_{k=0}^{N-1-|m|} z(n) z^*(n+m)$$

AR modelling

We replace the estimated correlation to the true one and we solve the linear system

$$\hat{\mathbf{a}} = \hat{\mathbf{R}}^{-1}\hat{\mathbf{r}}$$

so obtaining an estimate of the characteristic parameters of the PSD.

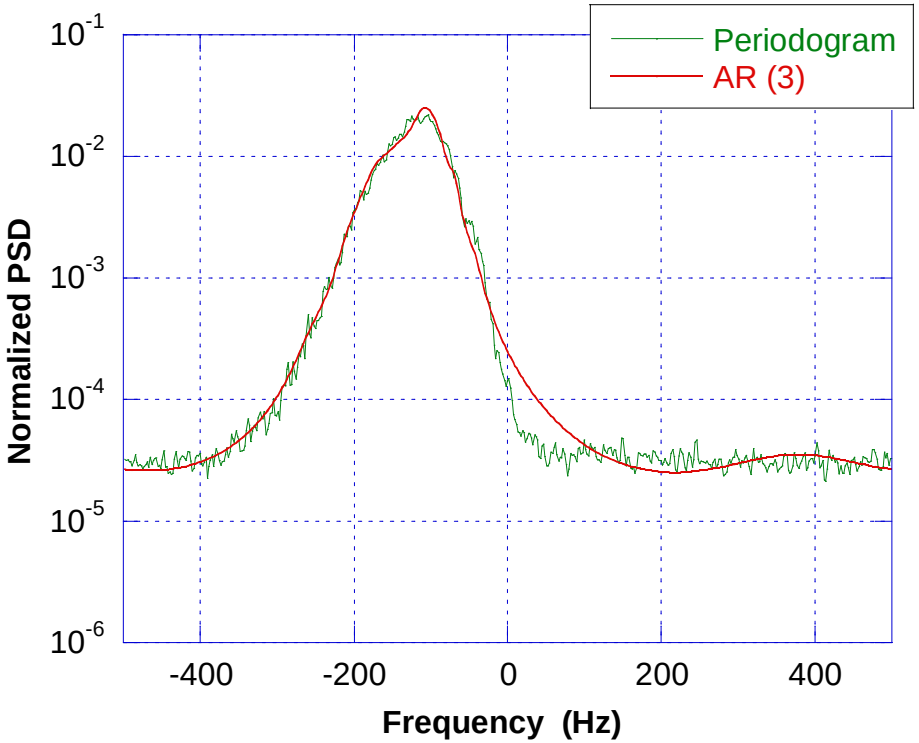

We tried AR(P) with P=1 up to 16.

AR(3) model shows good fitting with data and seems to capture physical phenomena.

Good compromise between model complexity and fitting accuracy.

Example of periodogram calculated on 60,000 HH polarized data.

Ground clutter data

PHASE ONE radar parameters

Source: MIT-LL, courtesy Mr. J. B. Billingsley

• Frequency Band (MHz)	VHF	UHF	L-Band	S-Band	X-Band
	165	435	1230	3240	9200
• PRF	500 Hz				
• Polarization (TX/RX)	VV or HH				
•Range Resolution	150, 36, 15 m				
•Azimuth Resolution	13°	5°	3°	1°	1°
•Peak Power	10 KW (50 KW at X-Band)				
•Antenna Control	Step or Scan through Azimuth Sector				
•Tower Height	60´ or 100´				
•10 Km Sensitivity	-60 dB				
•Amount of Data	25 Tapes/Site				
•Acquisition Time	2 Weeks/Site				

X-band ground clutter data in open agricultural terrain

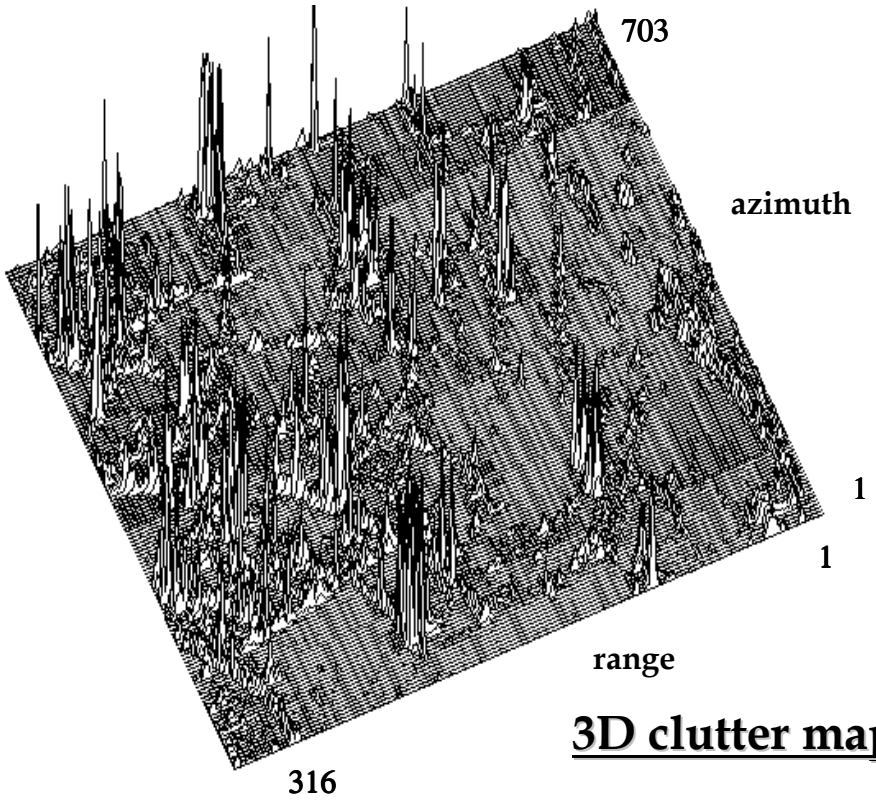

3D clutter map

VV polarization

The illuminated area was covered by agricultural crops (83%), deciduous trees (11%), lakes (4%), and rural farm buildings (2%).

2D clutter map

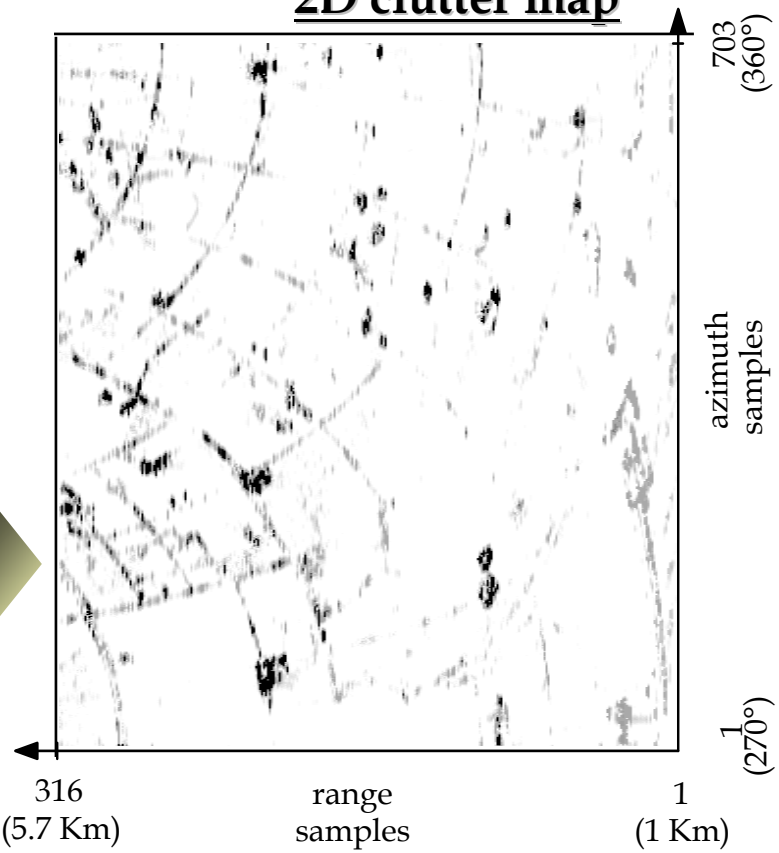

Black areas: high reflectivity (buildings, fencelines, trees, bushes aligned along roads)

White areas: low reflectivity (field surfaces)

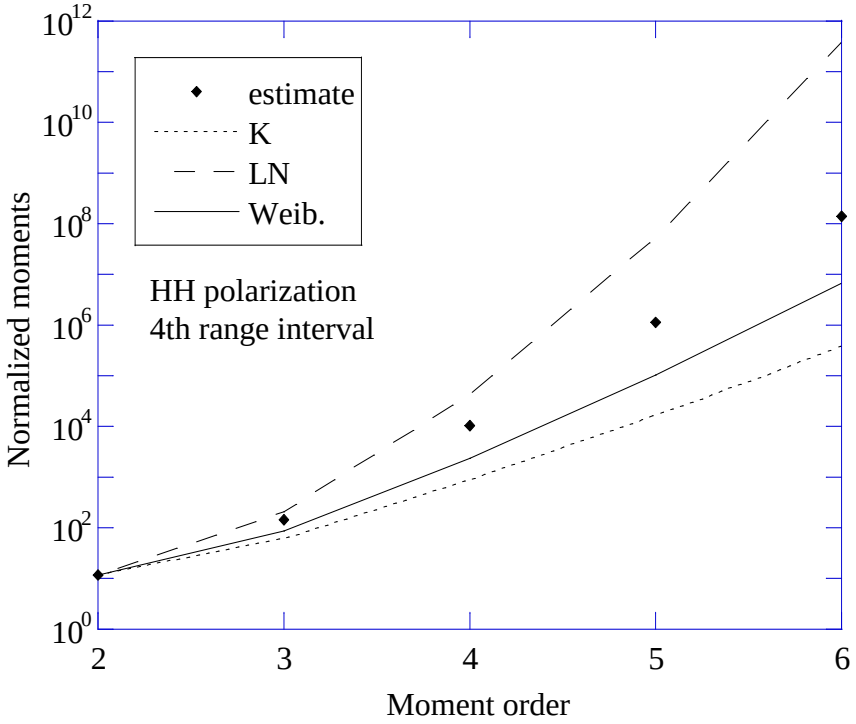

1st and 2nd range intervals:
the Weibull distribution
provides the best fitting

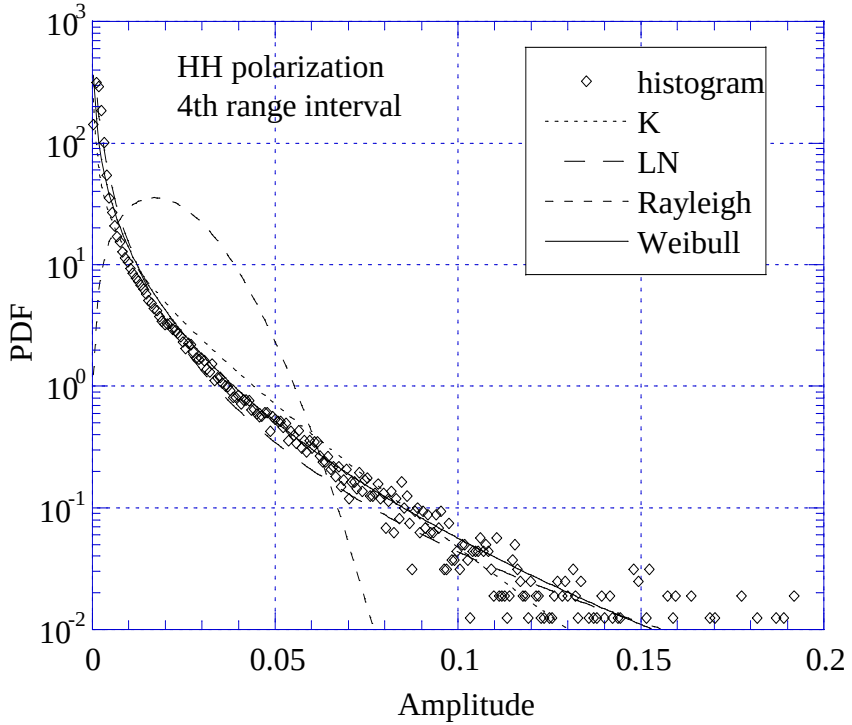

3rd and 4th range intervals:
the data show a behaviour that
is intermediate between
Weibull and log-normal

Ground clutter data analysis: windblown vegetation

Analyzed clutter data:

- recorded at Katahdin Hill site by Lincoln Laboratory.
- Phase One X-band stationary antenna.
- HH-polarization, PRF=500 Hz, 76 range gates.

3D power map

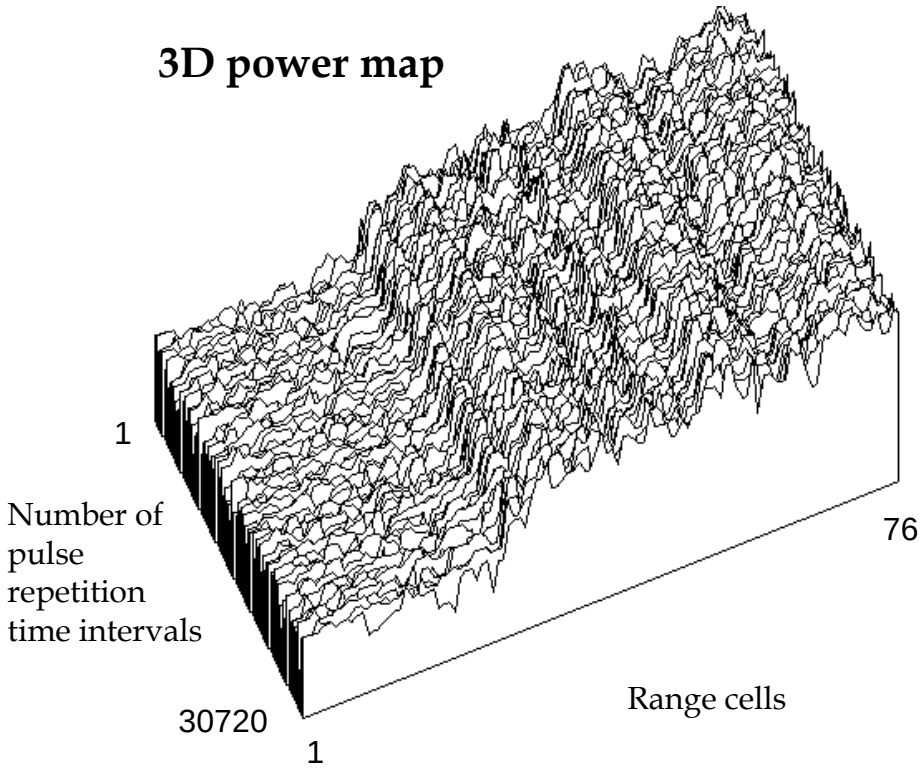

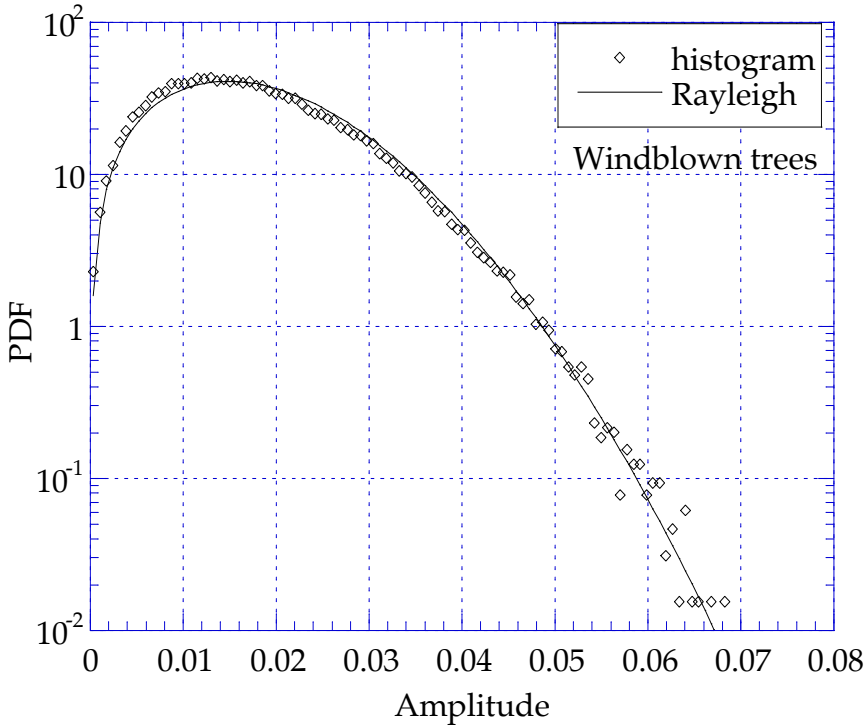

Data set courtesy of Barrie Billingsley of MIT – Lincoln Laboratory

These data are Gaussian.

Spectral model on windblown vegetation

PSD, 35th range cell.

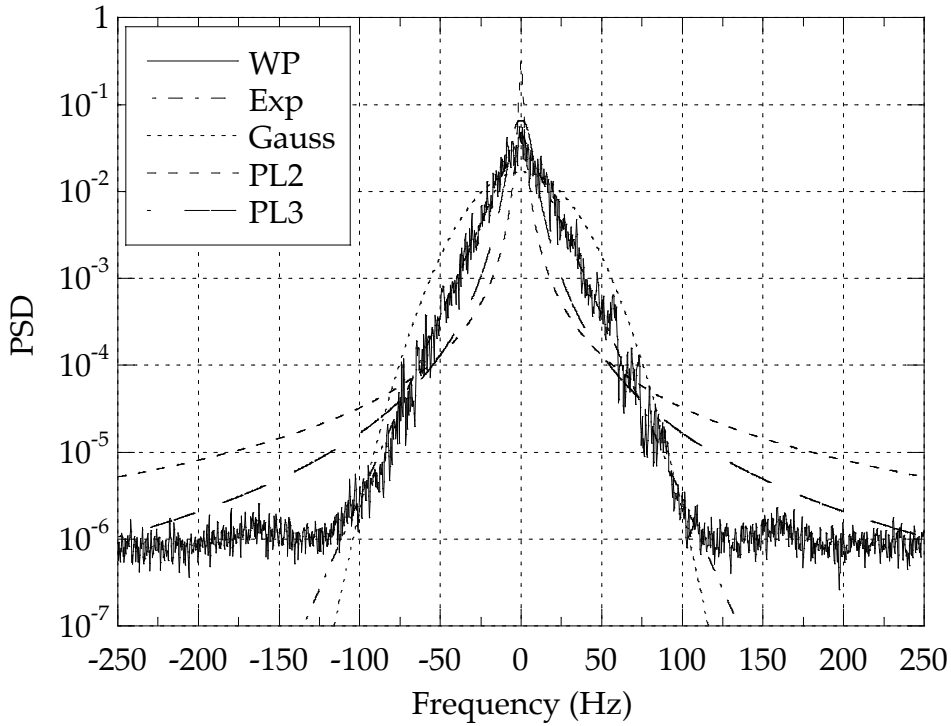

Cell #35	Exp	Gauss	PL2	PL3
$\beta/\sigma/f_c/f_c$	5.95 (Hz m)$^{-1}$	23.63 Hz	1.02 Hz	6.33 Hz

Non-Linear Least Squares (NLLS) method is used for parameter estimation:

$$\theta_{Log-NLLS} = \arg\min_{\theta} \sum_{i} \left| Log_{10} P_{ac}(f_i, \theta) - Log_{10} S(f_i) \right|^2$$